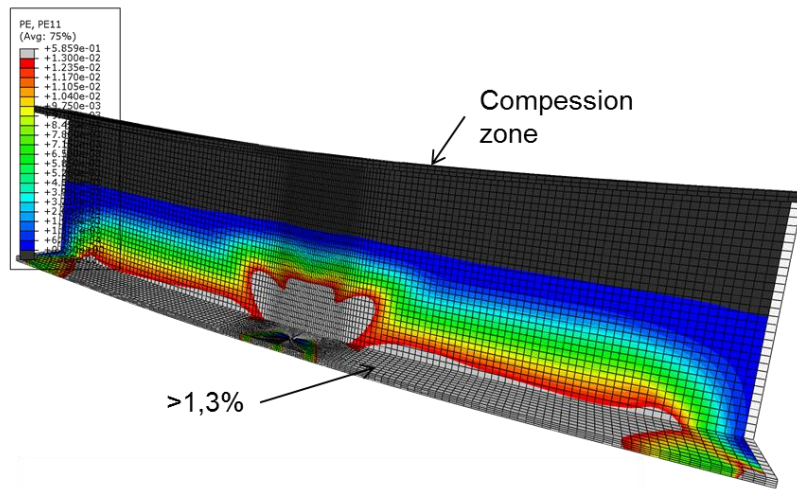


RESEARCH REPORT




VTT-R-02326-16



FEM based virtual testing of HSS beams with flange holes

Authors: Asko Talja, Juha Kurkela, Petr Hradil

Confidentiality: Public

Report's title	
FEM based virtual testing of HSS beams with flange holes	
Customer, contact person, address	Order reference
Finnish Metals and Engineering Competence Cluster (FIMECC)	BSA P2 SP2 Task 4
Project name	Project number/Short name
Virtual testing lab for novel materials and products	104679-1.2.3/VILMA
Author(s)	Pages
Asko Talja, Juha Kurkela, Petr Hradil	58 p.
Keywords	Report identification code
steel, beam, cross section, classification, FEM, Eurocode	VTT-R-02326-16
Summary	
<p>Material ductility requirements of beams with flange holes were verified by FEM based virtual testing. The study is based on a beam with a flange hole and uniform bending moment. Local buckling of the compressed parts was prevented by restraints. Tri-linear stress-strain material behaviour with (1) elastic stage up to yield stress f_y, (2) strain-hardening stage up to ultimate strength f_u and (3) ideal plastic stage after f_u was used in terms of true stresses and strains. Materials with f_u/f_y from 1.02 to 1.30 and ϵ_u from 2 to 10%, and yield strengths of $f_y = 1000$ MPa and $f_y = 500$ MPa were under consideration. Conditions for the cross section classification in Eurocodes were used as the basis of the study.</p> <p>The results indicate that in the case of usual I beams and hollow sections conditions $\epsilon_u \geq 6\epsilon_y$ and $A5 \geq \epsilon_u + 6\%$ result in adequate rotation capacity of Class 1 and Class 2 cross sections. Uniform elongation ϵ_u corresponds to the ultimate strength f_u and $\epsilon_y = f_y/E$. $A5$ is the elongation at failure with gauge length $5.65 \sqrt{A}$.</p> <p>In the case of beams with flange holes and Class 1 cross section an additional condition $M_u \geq 1.1 M_{pl}$ is required. Ultimate bending resistance M_u is determined by the net cross-section and ultimate strength f_u. Plastic bending resistance M_{pl} is calculated by the gross cross-section and yield strength f_y.</p> <p>The results indicate that Eurocode requirements are too conservative for beams with flange holes. In Eurocodes the material requirements are for uniform elongation $\epsilon_u \geq 15\epsilon_y$ and for fracture elongation $A5 \geq 10\%$. Also the requirement concerning the fastener holes in the tension flange of Class 1 cross sections seem to be too conservative.</p>	
Confidentiality	Public
Espoo 22.9.2016	
Written by	Reviewed by
 Asko Talja Senior Scientist	 Ludovic Fulop Principal Scientist
	Accepted by
	 Pekka Pohjanne Research Manager
VTT's contact address	
P.O. Box 1000, FI-02044 VTT, Finland	
Distribution (customer and VTT)	
Online at VTT research database (http://www.vtt.fi/haku)	
Online at FIMECC Research Portal	
<p><i>The use of the name of the VTT Technical Research Centre of Finland (VTT) in advertising or publication in part of this report is only permissible with written authorisation from the VTT Technical Research Centre of Finland.</i></p>	

Contents

1. Introduction.....	3
2. Theoretical study of material ductility for beams without holes	7
2.1 Rotation capacity	7
2.2 Plastic moment resistance	9
2.3 Code provisions for material ductility.....	11
3. Determination of rotation capacity.....	11
3.1 Testing methods	11
3.2 Four-point bending test.....	12
3.3 Rotation capacity in the case of a localised plastic hinge.....	13
3.4 Required rotation capacity – an example based on localized failure	15
3.5 Required rotation capacity – plastic collapse	16
4. Code provisions for member resistance	17
4.1 Members in bending	17
4.2 Members in tension	18
5. Preliminary study for I beam with real material properties	19
5.1 Input data	19
5.2 Moment-rotation behaviour	20
5.3 Rotation capacity	24
5.4 Effect of beam length on the rotation capacity	30
6. I beam with virtual material properties.....	30
6.1 Material data.....	30
6.2 Moment-rotation behaviour	32
7. Centre hole tension specimens with virtual material properties	39
7.1 Material data.....	39
7.2 Force-displacement behaviour.....	40
8. Material ductility requirements for the validity of the results.....	49
9. Summary and conclusions	51
9.1 Test matrix for virtual testing.....	51
9.2 Verification of net and gross cross section resistances	51
9.3 Verification of rotation capacity	54
9.4 Main conclusions	56
9.5 Some remarks on the results	57
References.....	57

1. Introduction

In the plastic design of structures, ductility is defined as the capacity of a structure to undergo deformations after reaching its initial yield without any significant reduction in ultimate strength. The ductility of a structure allows prediction of the ultimate capacity of a structure which is the most important criteria for designing structures under ultimate loads.

The inelastic behaviour of a structure depends upon the amount of moment redistribution. The attainment of the predicted collapse load is strictly related not only to the hinge position where the sections reach the full plastic moment M_p , but also to the inelastic rotation of other hinges elsewhere (Shokouhian & Shi 2014).

The following ductility types are widely used (Gioncu 2000, Figure 1 and Figure 2):

- material ductility, or axial ductility, which characterizes the material plastic deformations
- cross-section ductility, or curvature ductility, which refers to the plastic deformations of cross-section, considering the interaction between the parts composing it
- member ductility, or rotation ductility, when the properties of a member are considered
- structural ductility, or displacement ductility, which considers the behaviour of the whole structure.

In Figure 1 the subscript u refers to the ultimate deformation (strain, curvature, rotation or displacement), while subscript y indicates the corresponding deformation for first yielding. Referring to the ultimate deformation, the collapse of an element can be reached by plastic deformations limited by buckling or by fracture of some components. So, the ductility can be

- deformation ductility, when the collapse is due to buckling of a compressed element, or
- fracture ductility, when the collapse is the result of the fracture of a tensioned element.

This study focuses on the cross section ductility, and the study is based on the fracture ductility of different steel grades. Usually in limit design of structures it is required that plastic hinges have a sufficient rotation capacity, which is based on the occurrence of local buckling of plate elements in the member cross-section (Figure 2). However, local buckling is excluded from this study.

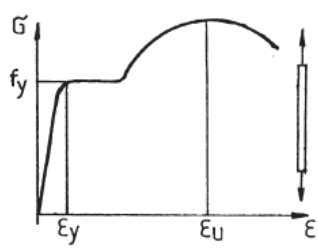
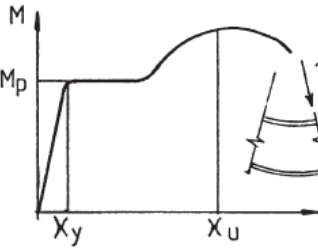
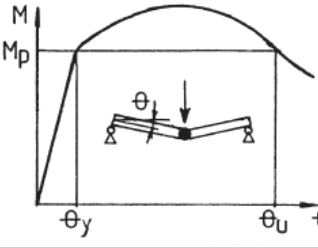
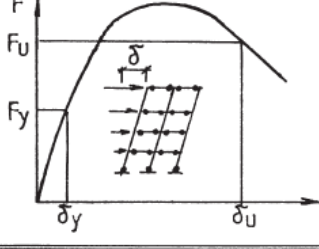
Ductility types	Schematic representation	Definition
Material (axial) ductility		$\mu_\varepsilon = \frac{\varepsilon_u}{\varepsilon_y}$
Cross-section (curvature) ductility		$\mu_\chi = \frac{\chi_u}{\chi_y}$
Member (rotation) ductility		$\mu_\theta = \frac{\theta_u}{\theta_y}$
Structure (displacement) ductility		$\mu_\delta = \frac{\delta_u}{\delta_y}$

Figure 1. Different type of ductility (Gioncu 2000). First two cases are based on material ductility of tensioned parts of the cross section, third one on the stability of compression parts of the member, and the last one on member and connection ductility of a frame.

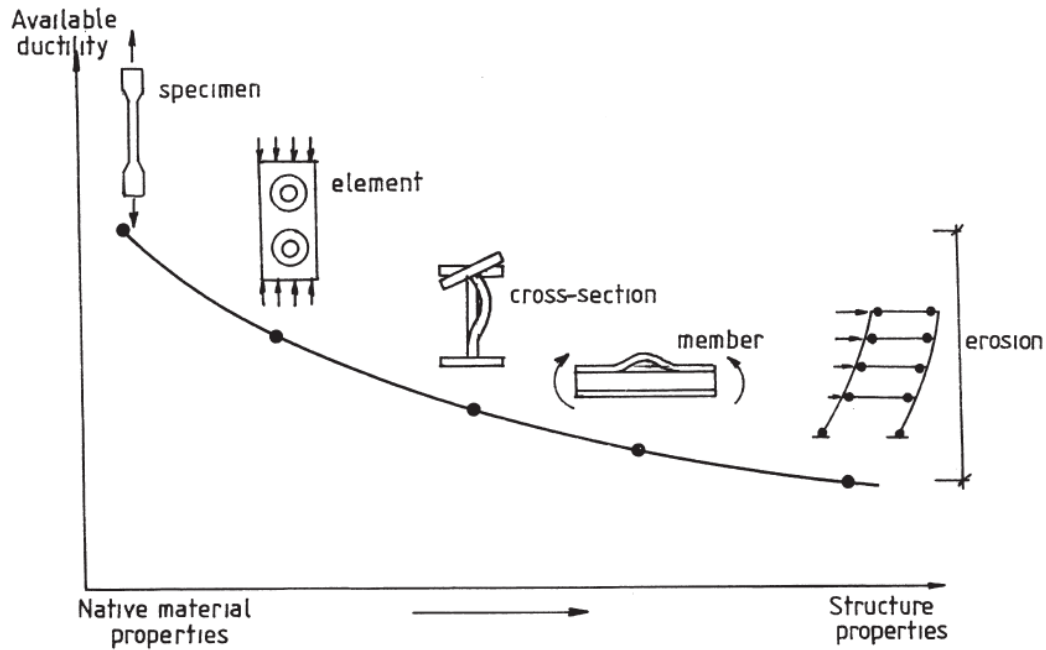


Figure 2. Different structural factors effect on the structure ductility (Gioncu 2000).

Section ductility of a steel section is usually defined as the ratio μ_x between the curvature which leads to the maximum moment χ_{max} and the curvature corresponding to plastic moment χ_p

$$\mu_x = \frac{\chi_{max}}{\chi_p}$$

Most usually section ductility is used for the classification of cross sections based on the plate buckling of the cross section, not for material ductility as in our case. The differences among cross section classes are governed by the element slenderness, defined by the width-to-thickness ratio.

In Eurocode approach the definition of the section ductility is related to the fully plastic moment (Figure 3 (b)). The rotation capacity is determined in the descending post-buckling curve at the intersection with the theoretical full plastic moment M_p . This definition is given in the Background Document 5.02 of Eurocode 3. In the Background Document of Eurocode 8 (earthquake design) there is also a proposal to use a reduced plastic moment $M_p/1.1 \approx 0.9 M_p$, which leads to an increase in ultimate rotation values (Gioncu & Petcu 1997, Shokouhian & Shi 2014).

In Eurocode 3 (RFCS1998) the formula calculating the available rotation capacity is given as

$$R = \mu_\theta = \frac{\theta_{rp}}{\theta_p} = \frac{\theta_r - \theta_p}{\theta_p} = \frac{\theta_r}{\theta_p} - 1$$

where θ_{rp} is the ultimate plastic rotation, θ_p is the rotation corresponding to the formation of the plastic hinge and θ_r is the total ultimate rotation (see Figure 3 (b)).

During some loading conditions of experimental tests the yielding plateau can occur under the reference value M_p . Therefore the above definition of rotation capacity cannot be used. For this case the rotation capacity can be determined for a reduced plastic moment $0.9 M_p$. Based on Eurocode 8 proposal (Gioncu & Petcu 1997) the rotation capacity is then

$$R_{0.9} = \mu_{\theta 0.9} = \frac{\theta_{r0.9}}{\theta_p} - 1$$

According to (Gioncu & Petcu 1997, Shokouhian & Shi 2014) also two other definitions have been proposed. Some researchers have proposed that the ultimate rotation should be based on the maximum moment with different levels of $0.8-0.95 M_{max}$ (Figure 3 (a)). The rotation capacity can also be considered in a more general way, in which, in addition to the rotation, the slope of the descending part of the moment-rotation curve is calculated (Figure 3 (c)).

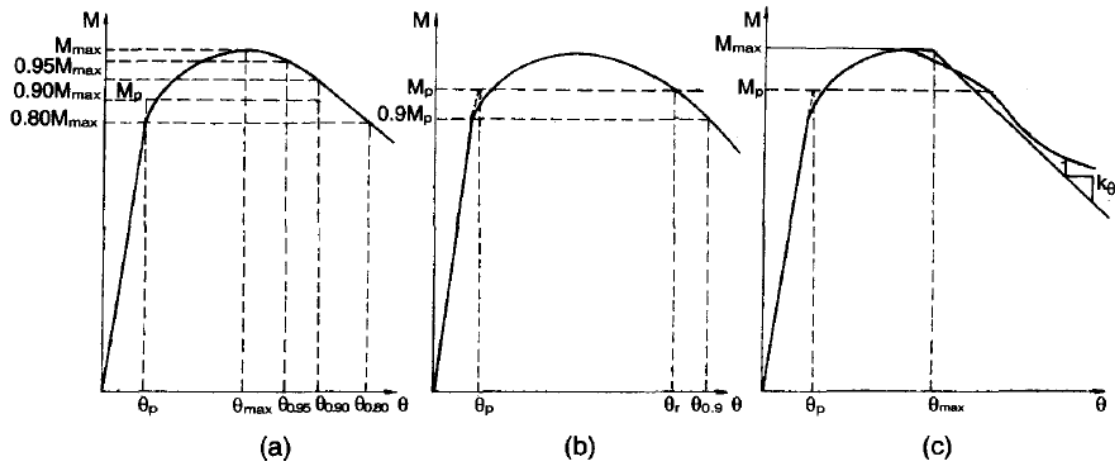


Figure 3. Different approaches to determine the rotation capacity (Gioncu & Petcu 1997).

In Eurocode 3 four classes of cross-sections are defined as follows (Figure 4, Figure 3b):

- Class 1 cross-sections are those which can form a plastic hinge with the rotation capacity required from plastic analysis without reduction of the resistance.
- Class 2 cross-sections are those which can develop their plastic moment resistance, but have limited rotation capacity because of local buckling.
- Class 3 cross-sections are those in which the stress in the extreme compression fibre of the steel member assuming an elastic distribution of stresses can reach the yield stress, but local buckling prevents development of the plastic moment resistance.
- Class 4 cross-sections are those in which local buckling will occur before the attainment of yield stress in one or more parts of the cross-section.

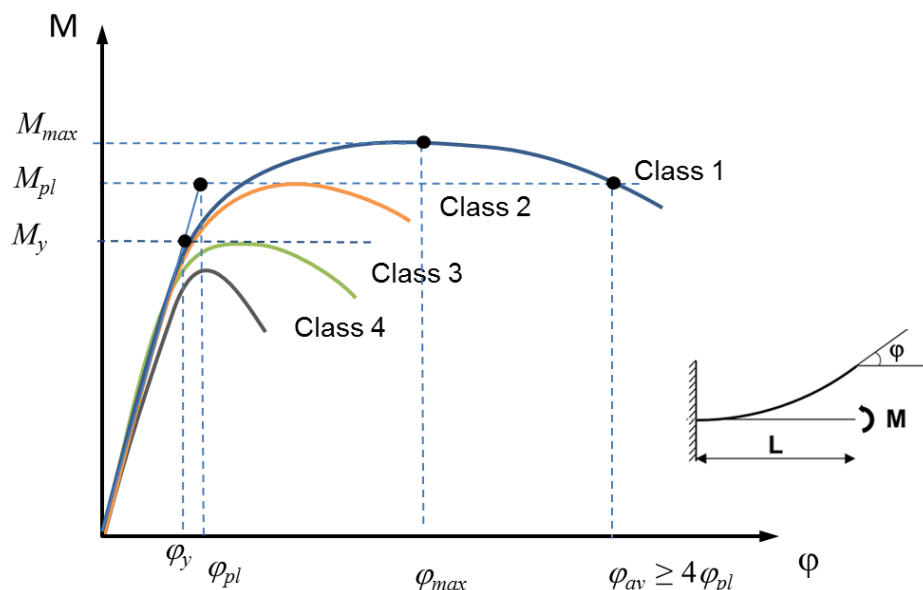


Figure 4. Cross section classes according to Eurocode 3.

Based on (Shokouhian & Shi 2014) the definitions of Classes 2 and 3 are clear. In the former case the girder must develop the plastic moment of the cross section (M_p), while in the latter the yield moment of the section (M_y). For the limit between Classes 1 and 2 some discrepancy exists between the codes in regard to the appropriate value of the rotation capacity. EC3 does not propose a certain value, stipulating that for Class 1 ‘sufficient’ rotation capacity must be available to allow for a plastic redistribution of the bending moments¹. The AISC LRFD specification states in the Commentary a value for the rotation capacity $R = 3$ for Class 1 sections, while the AIJ LSD Code (Japanese Recommendations on Limit State Design of Buildings) stipulates $R = 4$ (from Shokouhian & Shi 2014).

According to Shokouhian & Shi (2014) Mazzolani and Piluso (1997) have proposed classification criteria for members according to ductility classes:

- HD, high ductility, $\mu_{\theta r} \geq 7.5$
- MD, medium ductility, $4.5 \leq \mu_{\theta r} < 7.5$
- LD, low ductility, $1.5 \leq \mu_{\theta r} < 4.5$

where $\mu_{\theta r}$ is the rotation capacity of a flexural member.

2. Theoretical study of material ductility for beams without holes

Material ductility is necessary so that the requirements of Class 1 and Class 2 can be achieved. To be able to reach plastic moment resistance M_{pl} in Class 1 and Class 2 cross sections, the gain due to material strain hardening has to overcome the loss caused by the imperfect cross section plastification. Moreover, the condition of rotation capacity $R = 3$ for Class 1 cross sections assumes that the material can tolerate certain plastic deformations. For instance beam flanges should provide sufficient plastic deformation capacity to satisfy this condition. Eurocode 3 gives for the uniform elongation of material a requirement of $\varepsilon_u \geq 15\varepsilon_y$ ($\varepsilon_y = f_y/E$).

2.1 Rotation capacity

The deflection of a beam, which is loaded by end moments, is a circular arc with uniform axial strain distribution along its length. This is valid for uniform elongation until the ultimate strength of the material is reached and the necking in the tension flange starts. The load is typically rapidly decreasing beyond this point. Therefore we can conservatively assume that the rotation capacity is defined by the rotation at maximum load φ_{max} instead of φ_{av} (Figure 4). Then the end rotation of a symmetric cross section can also be expressed by means of beam curvature χ or by edge strain ε of the cross section (Figure 5).

$$\frac{\varphi_{max}}{\varphi_{pl}} = \frac{\varepsilon_{max}}{\varepsilon_{pl}} = \frac{\chi_{pl}}{\chi_{max}}$$

where φ_{max} , ε_{max} and χ_{max} refer to M_{max} , and φ_{pl} , ε_{pl} and χ_{pl} refer to M_{pl} in Figure 4.

¹ In addition to the previous, however, it has been found that rotation requirement $R = 3$ has also been used in Eurocode background documentation. The documentation has been presented in Annex 12 of reference (RFCS 1998)

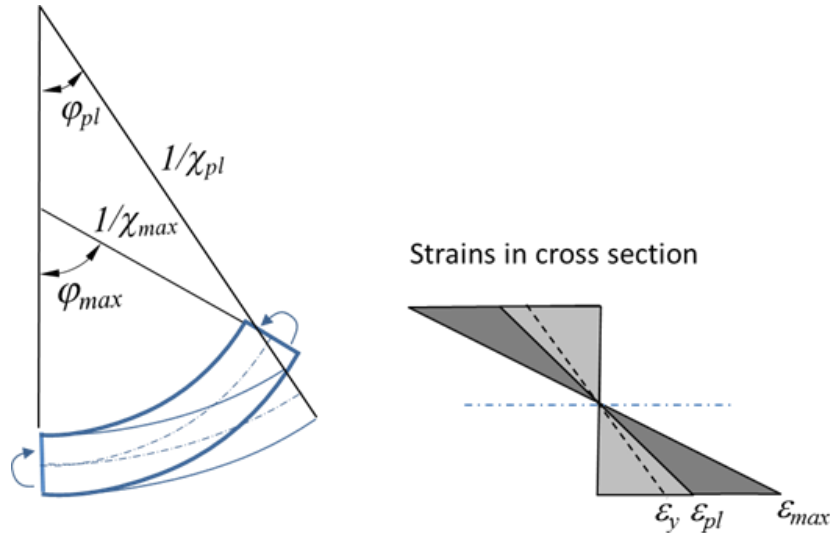


Figure 5. Strains in a partially plastified section of a beam subjected to uniform bending.

Because the plastic rotation in Figure 4 is defined as

$$\varphi_{pl} = \frac{M_{pl}}{M_y} \varphi_y = \frac{W_{pl}}{W} \varphi_y$$

the rotation capacity for $\varphi_{av} = \varphi_{max}$ can be expressed as

$$R = \frac{\varphi_{max}}{\varphi_{pl}} - 1 = \frac{W}{W_{pl}} \frac{\varphi_{max}}{\varphi_y} - 1 = \frac{W}{W_{pl}} \frac{\varepsilon_{max}}{\varepsilon_y} - 1$$

where $\varepsilon_y = f_y/E$. Then the condition for the uniform edge strain is

$$\frac{\varepsilon_{max}}{\varepsilon_y} \geq \frac{W_{pl}}{W} (R + 1)$$

Assuming that φ_{max} is achieved when $\varepsilon_{max} = \varepsilon_u$, the condition for material ductility corresponding to $R = 3$ can be presented as

$$\varepsilon_u \geq 4 \frac{W_{pl}}{W} \varepsilon_y$$

where the uniform elongation ε_u corresponds to the ultimate strength f_u on material stress-strain curve.

Table 1 shows the condition for selected cross sections. The table is determined using the centreline dimension of the cross section. Because the effect of plate thickness is omitted, the real values of min ε_u can be slightly higher than given in the table. The most conservative value of $\varepsilon_u = 6\varepsilon_y$ is valid if the cross section is a solid rectangle, or in the case of CHS if $d_1/d_2 > 0.65$. Therefore in the case of usual I beams and hollow sections with any shape the minimum uniform elongation of $6\varepsilon_y$ results in adequate ductility. For example in the case of $f_y = 1000$ MPa $6\varepsilon_y$ is 3%.

Table 1. Required minimum uniform elongation ε_u for some cross sections.

Cross section	W	W_{pl}	$\frac{W_{pl}}{W}$	min ε_u
I section without web	$bt_f \cdot h_w$	$bt_f \cdot h_w$	1.00	$4.0\varepsilon_y$
I section with $h_w t_w = bt_f$	$\frac{7bt_f \cdot h_w}{6}$	$\frac{5bt_f \cdot h_w}{4}$	1.07	$4.3\varepsilon_y$
RHS with $h_w = b$	$\frac{4bt \cdot h_w}{3}$	$\frac{3bt \cdot h_w}{2}$	1.13	$4.5\varepsilon_y$
RHS with $h_v = 3b$	$2bt \cdot h_w$	$\frac{5bt \cdot h_w}{2}$	1.25	$5.0\varepsilon_y$
CHS	$\pi r^2 t$	$4r^2 t$	1.27	$5.1\varepsilon_y$
CHS with $d_1/d_2 \geq 0.65$	$\frac{\pi(d_2^4 - d_1^4)}{32d_2}$	$\frac{(d_2^3 - d_1^3)}{6}$	≤ 1.5	$6.0\varepsilon_y$
Solid rectangle	$\frac{bh^2}{6}$	$\frac{bh^2}{4}$	1.5	$6.0\varepsilon_y$
Notations	t_f is flange thickness of I section t_w is web thickness of I section b is flange width of I section and RHS h_w is height I of section and RHS t is plate thickness of RHS and CHS r is centreline radius of CHS d_1 and d_2 are inner and outer diameter for CHS b and h are width and height for a solid rectangle			

2.2 Plastic moment resistance

The reduction of cross-section capacity caused by imperfect cross section plastification in the vicinity of the neutral axis has to be compensated by material strain hardening, in order to reach plastic moment resistance M_{pl} (Figure 6). In common double symmetric cross section the gain M^+ and loss M^- can be calculated from quarter of the section as:

$$M^- = 4 \int_0^{x_0} x \cdot \sigma^-(x) dA$$

and the gain can be determined as

$$M^+ = 4 \int_{x_0}^h x \cdot \sigma^+(x) dA$$

Stress distributions $\sigma^-(x)$ and $\sigma^+(x)$ are shown in Figure 6.

We assume a limit of the spread of plastic axial strain in the section (x_0 in Figure 5). Below that position in the section the stress distribution is $\sigma^-(x)$ which causes the loss in bending stress with value of $\sigma = f_y$ at $x = 0$ and $\sigma = 0$ at $x = x_0$. Above that position the stress distribution which causes the maximum possible gain in bending moment $\sigma^+(x)$ has value of $\sigma = f_y$ at $x = x_0$ and $\sigma = m \cdot f_y$ at $x = h$.

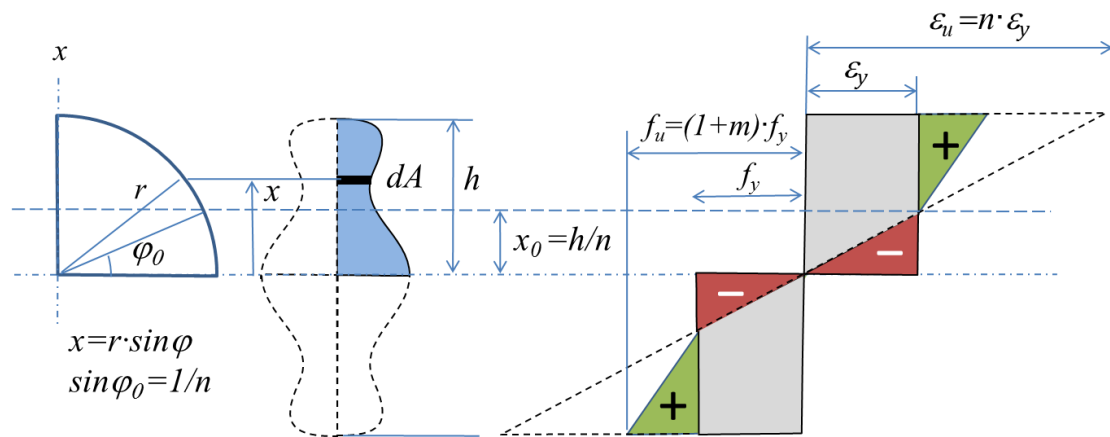


Figure 6. Effect of strain hardening on bending resistance.

Here it is conservatively assumed that the failure in tension flange occurs when the edge strain of the beam reaches the uniform elongation of the material. Table 2 shows the formulas for calculation the loss and gain for some sections. For simplifying the calculations the effect of ratios t_f/h and r/t is excluded.

Calculation results for some specific cross sections in Figure 7 show that the required uniform-to-yield elongation ratio ϵ_u/ϵ_y depends on the shape of the cross section and on f_u/f_y ratio. If f_u/f_y is at least 1.02, uniform elongation of $\epsilon_u \geq 6\epsilon_y$ is adequate for usual I beams and hollow sections. However, if f_u/f_y ratio is higher, also lower values of ϵ_u are making it possible to reach M_{pl} , the requirement for Class 2 cross sections.

Table 2. Maximum gain in bending resistance due to strain hardening and loss due to imperfect cross section plastification.

	RHS and symmetric I beam	CHS tube
M_{pl} for perfect plastification	$M_{pl} = 2h(A_f + \frac{A_w}{2}) \cdot f_y$	$M_{pl} = 4f_y r^2 t$
Loss due to imperfect plastification	$M^- = A_w f_y \frac{h}{3n^2}$	$M^- = 4f_y r^2 t \left[1 - \cos(\varphi_0) - \frac{\varphi_0}{2} + \frac{1}{4} \sin(2\varphi_0) \right]$
Maximum gain due to strain hardening	$M^+ = 2mf_y h \left[A_f + \frac{A_w}{6} \left(2 - \frac{1}{n} - \frac{1}{n^2} \right) \right]$	$M^+ = 4mf_y r^2 t \frac{1}{1 - \sin\varphi_0} \left[\frac{\pi}{4} - \frac{\varphi_0}{2} - \frac{1}{4} \sin(2\varphi_0) \right]$
Notations	$h = h_w/2$ (half height) $A_f = bt_f$ (flange area) $A_w = ht_w$ (half of web area) $m = f_u/f_y - 1$ $n = \epsilon_u/\epsilon_y$	$m = f_u/f_y - 1$ $n = \epsilon_u/\epsilon_y$ $\sin(\varphi_0) = 1/n$

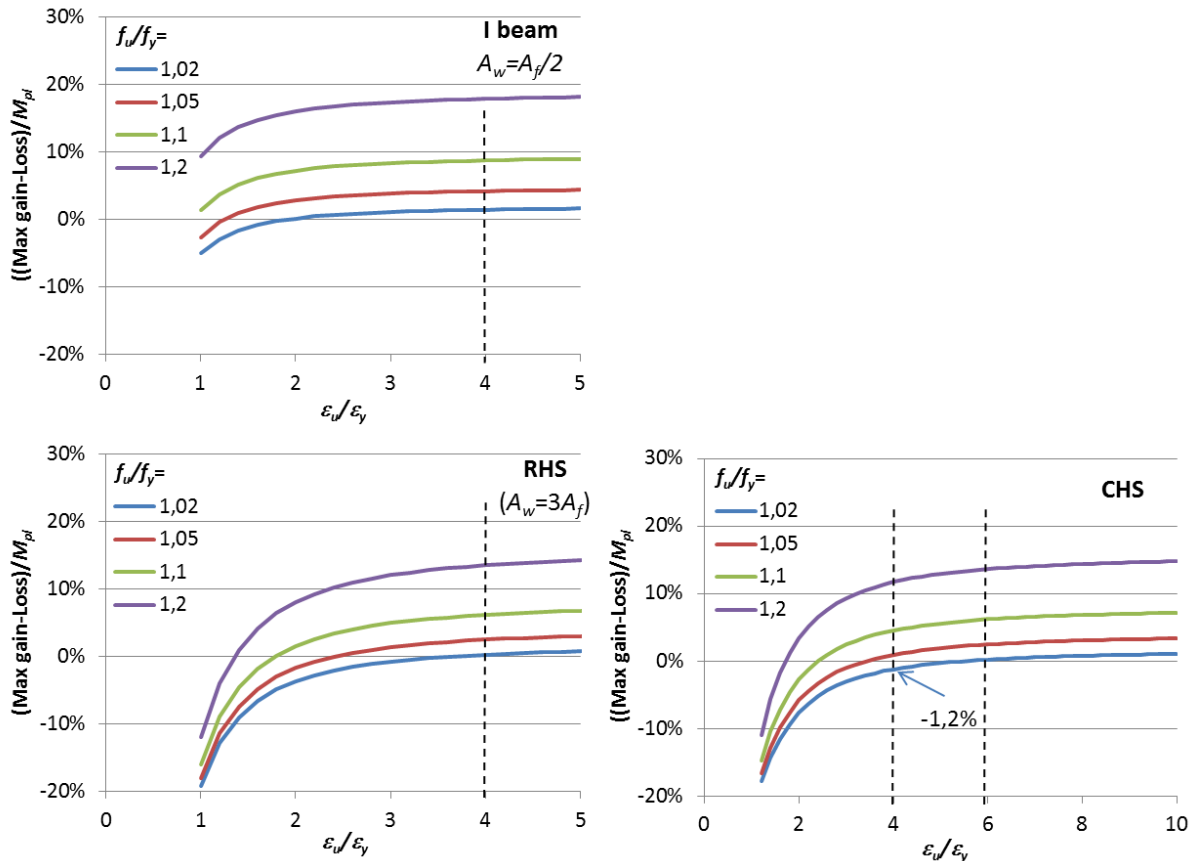


Figure 7. Relative gain in bending resistance due to material strain hardening.

2.3 Code provisions for material ductility

In rules of Eurocode 3 (EN1993-1-1), valid for steels up to grade S460, the material requirements are $f_u/f_y \geq 1.10$ and $\epsilon_u \geq 15\epsilon_y$, where ultimate strain ϵ_u corresponds to the ultimate strength f_u and ϵ_y is the yield strain ($\epsilon_y = f_y/E$). The elongation at failure shall be $A5 \geq 15\%$ ($L_0 = 5.65 \sqrt{A}$). For steel grades above S460 and up to S700 (EN1993-1-12) the material shall have $f_u/f_y \geq 1.05$ and $A5 \geq 10\%$, but the requirement for $\epsilon_u \geq 15\epsilon_y$ is identical.

In North American specification AISI S100 (2007) for cold-formed structural members the requirements are $f_u/f_y \geq 1.08$ and $A_{50} \geq 10\%$ ($L_0 = 50$ mm). If these requirements cannot be met, the local elongation across the fracture shall be $\geq 20\%$ in a 12.7 mm gauge length and the uniform elongation outside the fracture shall be $\geq 3\%$. Background for AISI approach is presented by Dexter & al. (2002).

3. Determination of rotation capacity

3.1 Testing methods

The rotation capacity (R) indicates how much the plastic hinge can rotate before the moment falls below the plastic moment resistance (M_{pl}) on the descending part of the moment-rotation curve.

The background for the rotation capacity is in utilization of plastic design in continuous beams (Figure 8). Therefore in Eurocode background documentation (RFCS 1998) three point bending test has been used to obtain the rotation capacity under moment gradient. However, there is mentioned that to obtain the rotation capacity of section with moments but without

moment gradient, four-point bending test may also be used. Four-point bending test has been used e.g. by Wilkinson & Hancock (1998) in determination of class 1 limits for rectangular hollow sections (Figure 9).

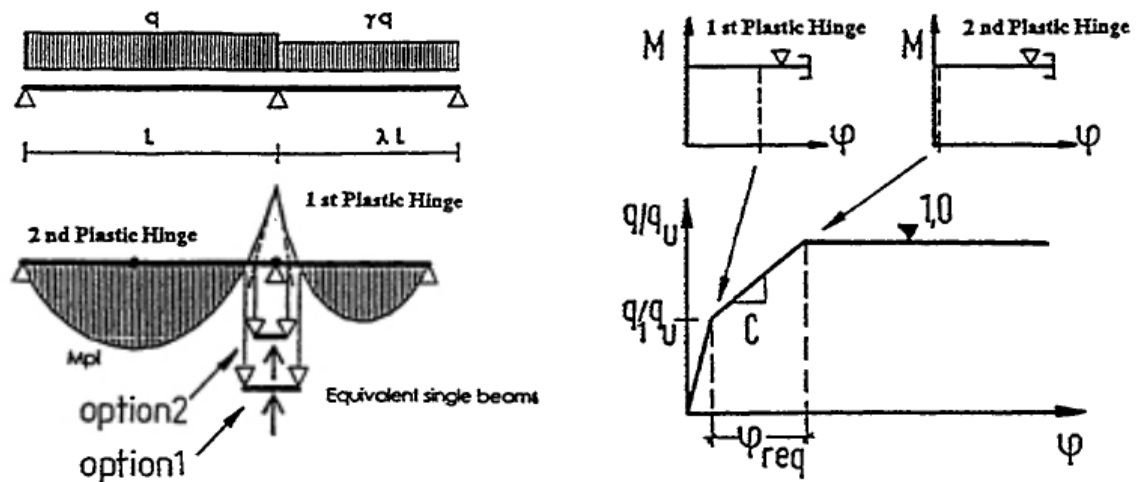


Figure 8. Obtaining the required rotation on support (RFCS 1998).

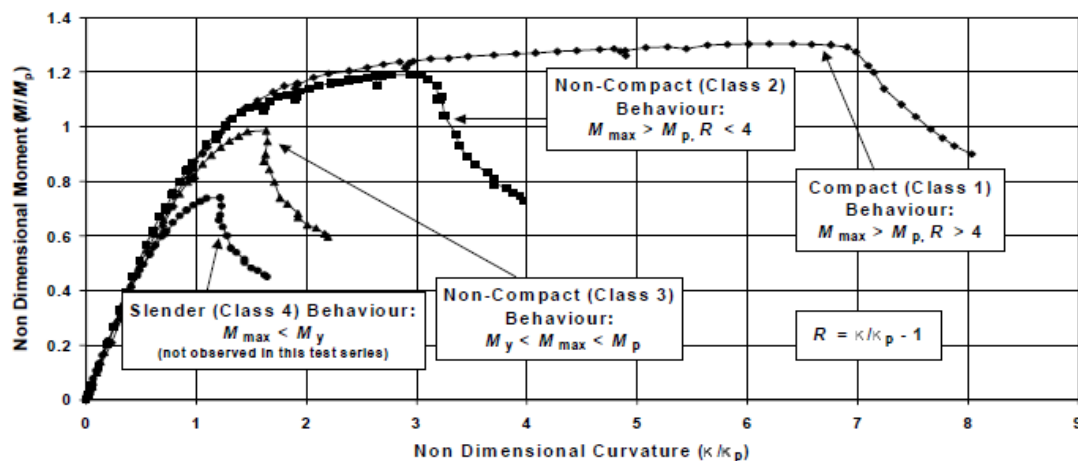


Figure 9. Non dimensional curvature χ/χ_{pl} of cold-formed RHS beams (Wilkinson & Hancock 1998).

3.2 Four-point bending test

The principle of the test is shown in Figure 10. The rotation capacity is expressed as

$$R = \frac{\chi}{\chi_{pl}} - 1$$

where χ/χ_{pl} is a non-dimensional curvature. Value of χ_{pl} in the non-dimensional curvature χ/χ_p is determined by

$$\chi_{pl} = \frac{M_{pl}}{EI} = \frac{W_{pl}f_y}{EI}$$

It is dependent only on material yield stress and cross-sectional properties. The beam curvature χ is based on measurement of displacements in three positions. The measuring points are positioned at the region of uniform bending moment. The measured curvature includes both elastic and plastic deformations.

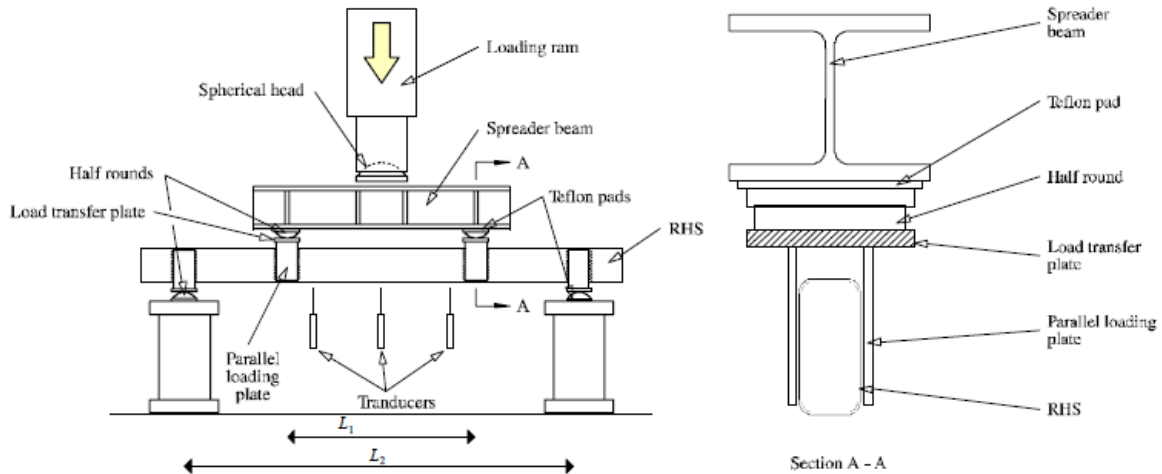
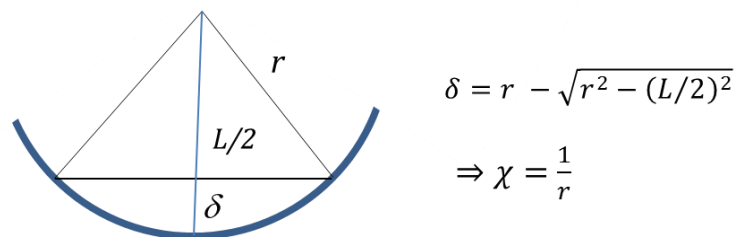


Figure 10. Determination of rotation capacity by four-point bending test (Wilkinson & Hancock 1998).

Because the curvature of a uniform beam under uniform bending is constant, the curvature can be determined based on a circular arc with radius $r = 1/\chi$ and deflection δ . The length of the arc is the distance L of the outermost measurement points. Based on the equation in Figure 11,

$$\chi = \frac{1}{r} = \frac{8\delta}{L^2 + 4\delta^2}$$



$$\delta = r - \sqrt{r^2 - (L/2)^2}$$

$$\Rightarrow \chi = \frac{1}{r}$$

Figure 11. Determination of the curvature based on measured difference of deflections.

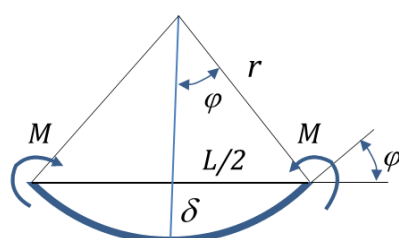
3.3 Rotation capacity in the case of a localised plastic hinge

The rotation capacity can be presented by the help of the end rotation φ (Figure 12). When the curvature of the beam is constant,

$$R = \frac{\varphi}{\varphi_{pl}} - 1$$

where the reference value for the rotation is defined as

$$\varphi_{pl} = \frac{M_p}{EI} \cdot \frac{L}{2} = \frac{W_p f_y}{EI} \cdot \frac{L}{2}$$



In the case of small rotations:

$$\varphi[\text{rad}] = \frac{L}{2r} = \chi \cdot \frac{L}{2} = \frac{M}{EI} \cdot \frac{L}{2}$$

Figure 12. The relationship between the curvature and end rotation.

If a plastic hinge with an angle of $\Delta\theta$ is formed in the middle of the beam (e.g. because of a large hole in flange, Figure 13), it increases the end rotation of the beam by $\Delta\theta/2$ (Figure 14).

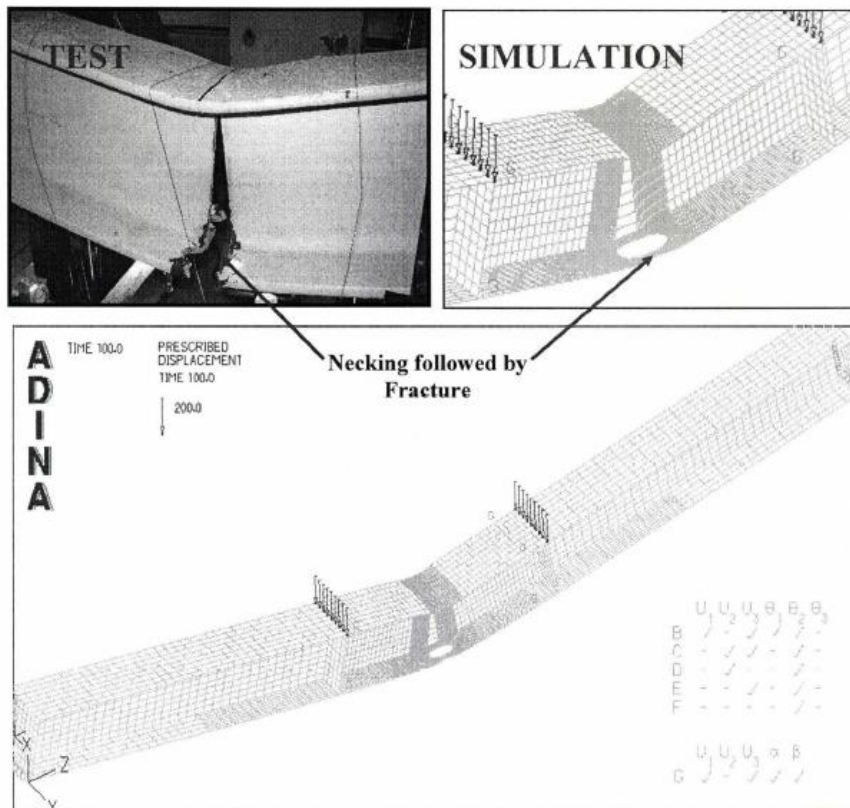


Figure 13. Local plastic hinge of a beam (Arasaratnam 2008).

In addition to the local angle, there exists also end rotation θ_{pl} due to the uniform curvature of the beam (Figure 14). Then the rotation capacity is

$$R = \frac{\theta_{pl} + \Delta\theta/2}{\varphi_{pl}} - 1$$

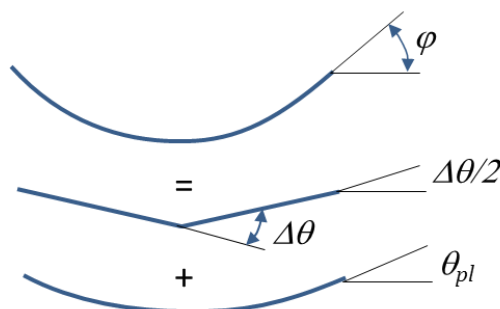


Figure 14. End rotation in the case of localized plastic hinge.

In the case of localized plastic hinges, θ_{pl} due to uniform curvature depends on the length of the beam but $\Delta\theta$ is independent on it. Therefore, with shorter length (L) the effect of a local hinge on the rotation capacity is increasing. Due to the localized failure, the rotation capacity is a subjective measure and it depends also on loading arrangements of the test (see also Arasaratnam 2008).

3.4 Required rotation capacity – an example based on localized failure

If we consider the case of a uniformly loaded continuous beam with a hinge forming on the support; and conservatively assume that the hinge does not take any bending moment (Figure 15). What kind of rotation capacity is necessary at the support, if the design is based on limited deflection or on initiation of yield at mid-span?

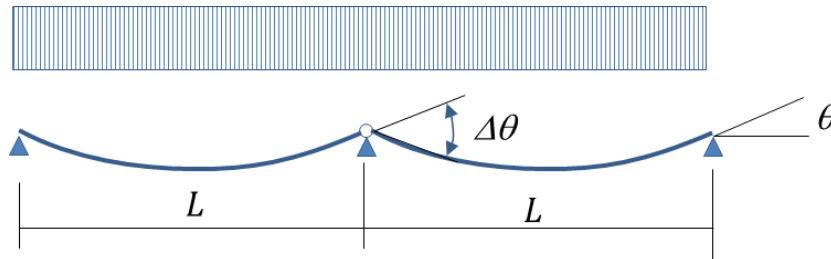


Figure 15. Rotations in the case of localized plastic hinge of a two-span beam.

Assuming that that determining factor in the design can be beginning of yield in the mid-span or mid-span deflection.

The deflection of a single span beam is

$$\delta = \frac{5FL^3}{384EI} = \frac{5FL^3}{16 \cdot 24EI} = \frac{5L}{16} \theta$$

where F is the load of one span. The end rotation (slope at the beam end) is

$$\theta = \frac{FL^2}{24EI} = \frac{16}{5} \frac{\delta}{L}$$

This is the maximum value of end rotation if L/h is large enough (Figure 16) and the design is limited by the deflection limit (δ/L). Otherwise the end rotation is smaller and it is determined based on the beginning of yield in mid-span.

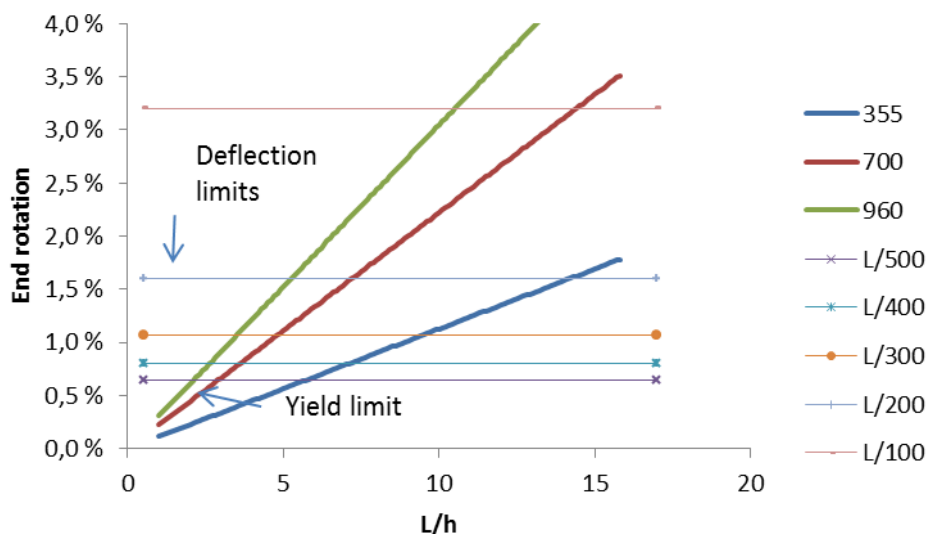


Figure 16. Limit for end rotation of a beam based on yield limits or deflection limits (steel grades S355, S700 and S960).

In the case of symmetric beam with height h , the deflection at the beginning of yield is (Figure 16)

$$\delta = \frac{5f_y L^2}{24Eh}$$

$$\Rightarrow \theta = \frac{16\delta}{5L} = \frac{2f_y L}{3Eh}$$

The required rotation at the mid-support is double to the end rotation

$$\Delta\theta = 2\theta = \frac{32}{5} \cdot \frac{\delta}{L}$$

Based on the deflection limit (δ/L), to reach such a rotation, the difference of elongations of top and bottom flanges shall be

$$\Delta l = \Delta\theta \cdot h = \frac{32}{5} h \cdot \frac{\delta}{L}$$

$$\Rightarrow \frac{\Delta l}{h} = \frac{32}{5} \cdot \frac{\delta}{L} = 6.4 \cdot \frac{\delta}{L}$$

If e.g. deflection limit $L/200$ is used in the structural design, the required difference in elongation of flanges is $\Delta l = 0.032h$. In the case of $h = 600$ mm that means axial deformation of 9.6 mm in both flanges. The beam has to tolerate these local deformations without failure.

It should be noted that the end rotation in the case of uniform bending, based on deflection limit, is a little bit higher than in previous study. Then

$$\theta = 4 \frac{\delta}{L}$$

and then in the case of deflection limit the difference of elongations of top and bottom flanges shall be

$$\Rightarrow \frac{\Delta l}{h} = 8 \cdot \frac{\delta}{L}$$

3.5 Required rotation capacity – plastic collapse

A good literature review on background of rotation capacity is presented by Wilkinson (1999) which is referred below. In plastic design the already formed plastic hinges must be able to rotate a certain amount to redistribute the bending moment.

Kerfoot (1965) analysed three span beams with point loadings. It was found that only in extreme cases would a plastic hinge rotation greater than $M_{pl}L/EI$ be needed to form a plastic collapse mechanism (L is the length of each span). For $I/W = h/2$, $M_{pl}L/EI = (f_y/E)(2L/h)$. That means that the required hinge rotation depends also on the material strength in the case of plastic collapse.

Driscoll (1958) considered three span beams (each span of length L) with distributed loads. It was shown that a plastic hinge rotation of $0.425 M_{pl}L/EI$ was the maximum required for the three-span beam. Driscoll extended the analysis to frames. For a single span rigid frame (Figure 17) $0.475 M_{pl}L/EI$ was the required plastic hinge rotation, and for gable frames (pitched roof) $1.05 M_{pl}L/EI$ was the maximum required plastic hinge rotation.

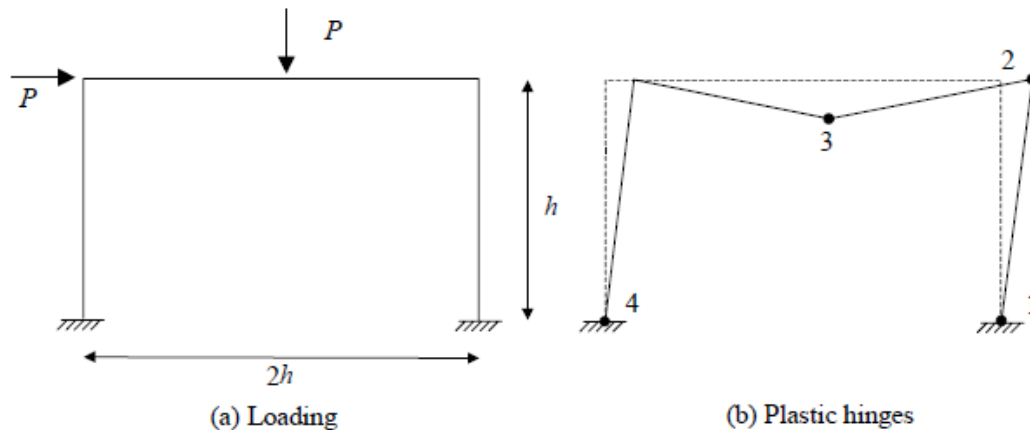


Figure 17. Plastic hinges in a simple portal frame (Wilkinson 1999).

Since the rotation capacity requirements vary according to the loading and geometry of the structure, it is convenient to establish a representative value of rotation capacity that covers most common practical situations. The Eurocode 3 Editorial Group (1989) summarise the rotation requirements for a variety of frames and multi-span beams constructed from I sections and concluded that a value of $R = 3$ was a suitable value to ensure that a plastic collapse mechanism could form. The value of $R = 3$ is therefore used in Eurocode 3.

Yura, Galambos and Ravindra (1978) state that the AISC LRFD specification is also based on $R = 3$. AISC LRFD states, in Commentary to Clause B.5, that in seismic regions greater rotation capacity may be required that the rotation provided by a compact section, and rotation capacities of the order $R = 7 \sim 9$ (Chopra and Newmark 1980) need to be provided.

Korol and Hudoba (1972) considered hollow sections and recommended that a value of $R = 4$ was the minimum necessary to ensure that a plastic mechanism could form. Hasan and Hancock (1988) and Zhao and Hancock (1991) followed the suggestion of Korol and Hudoba, and used the value of $R = 4$, for determining suitability for plastic design in the establishment of values for the Australian Standard AS 4100.

4. Code provisions for member resistance

4.1 Members in bending

According to Eurocode, for beams with Class 1 and Class 2 cross sections, the design resistance shall be greater than

$$M_{c,Rd} = \frac{W_{pl}f_y}{\gamma_{M0}}; \gamma_{M0} = 1.0$$

Each cross-section of the beam shall fulfil the above condition. Therefore, for net section resistance $W_{pl,net}$ can be used in the equation. In that case internal forces and moments may be calculated according to elastic global analysis; however the section check is still carried out using plastic resistance (RFCS 1998).

Concerning the fastener holes in the tension flanges of beams, the holes may be ignored provided that for the tension flange

$$\frac{0.9A_{f,met} f_u}{\gamma_{M2}} \geq \frac{A_f f_y}{\gamma_{M0}}$$

Note that the condition is not required for cross-sections if the global analysis is elastic; it is required only in capacity design of Class 1 cross sections in a plastic global analysis. A cross section requirement for plastic global analysis is that the member has Class 1 cross-section at the plastic hinge location and that adjacent to a plastic hinge location any fastener holes in tension satisfy the condition above.

In AISC (2010) the holes in tension flange of beams may be ignored provided that for the tension flange

$$A_{f,net}f_u \geq Y_t A_f f_y$$

where $Y_t = 1$ for $f_y/f_u \leq 0.8$, else $Y_t = 1.1$. Otherwise the moment resistance is determined by

$$M_n = \frac{A_{f,net}}{A_f} f_u W$$

where W is elastic section modulus.

4.2 Members in tension

According to Eurocode, the design resistance in tension is based on the plastic resistance of the gross cross-section ($N_{pl,Rd}$) and ultimate resistance of the net cross-section at holes for fasteners ($N_{u,Rd}$). Design resistance shall be taken as the smaller of $N_{pl,Rd}$ and $N_{u,Rd}$.

$$N_{pl,Rd} = \frac{A f_y}{\gamma_{M0}}; \gamma_{M0} = 1.0$$

$$N_{u,Rd} = \frac{0.9 A_{net} f_u}{\gamma_{M2}}; \gamma_{M2} = 1.25$$

Where capacity design (EN1998) is requested, the design plastic resistance $N_{pl,Rd}$ should be less than the design ultimate resistance of the net section at fasteners holes $N_{u,Rd}$. This results in the following condition for capacity design

$$A_{net} \geq \frac{1.25 f_y}{0.9 f_u} A = 1.39 \frac{f_y}{f_u} A$$

In AISC Specification (AISC 2010) the corresponding resistances are determined by

$$F_y = 0.9 A_g \cdot f_y$$

$$F_u = 0.75 A_{net} \cdot f_u$$

Based on AISC equations the condition for the yield of gross cross section is

$$A_{net} \geq 1.20 \frac{f_y}{f_u} A_g$$

This means that the Eurocode requirement is more conservative than the AISC requirement.

5. Preliminary study for I beam with real material properties

5.1 Input data

The case study is made to describe the influence of material properties on the moment rotation behaviour. One I beam (Figure 18, height 256 mm, width 164 mm) made of four different materials (Table 3, Figure 19) has been compared. The tension flange has a small hole on both sides of the web. In addition to the beam without holes, two diameters with hole sizes 8 mm and 16 mm are studied. The length of the beam is 1000 mm except of some preliminary studies with length of 500 mm. Both ends are modelled infinitely stiff and the beams are loaded by end rotation, resulting in uniform bending moment along the beam. Because only the material ductility is under consideration, the buckling of the compressed flange is prevented by forcing it to remain in the horizontal plane. One quarter of the beam (length $L = 500$ mm), using symmetry conditions, was modelled by Abaqus.

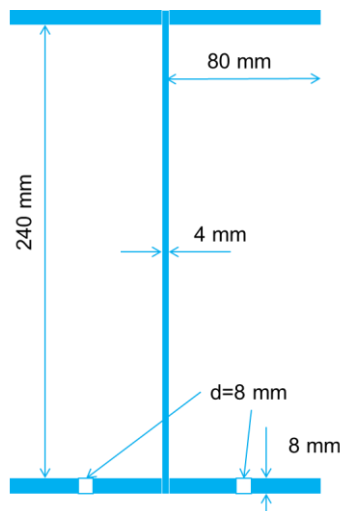


Figure 18. Cross-sectional dimensions and material thicknesses used in modelling.

Table 3. Material properties based on tensile testing of coupons.

	t (mm)	b (mm)	f_y (MPa)	f_u (MPa)	E (GPa)	f_u/f_y	$\varepsilon_u (A_{gt})$	ε_f	$\varepsilon_{eq,f}$
S960	8.07	20.12	1062	1167	210	1.10	3.0%	9.8 % (A_{80})	98%
S700	10	20	708	792	210	1.12	9.5%	20.6% (A_5)	114%
S355MC	7.97	25	397	473	210	1.19	17.6%	31.3% (A_5)	141%
S355J2	9.98	19.8	393	550	210	1.40	13.4%	28.1% (A_5)	138%
	t – material thickness b – specimen width f_y – upper yield strength or 0.2% proof stress f_u – ultimate tensile strength E – Modulus of elasticity					$\varepsilon_u (A_{gt})$ – percentage of total elongation at maximum load (gauge length A_5 or 80 mm) ε_f – percentage of total elongation at fracture $\varepsilon_{eq,f}$ – maximum equivalent plastic (true strain) at fracture (FEM calculation)			

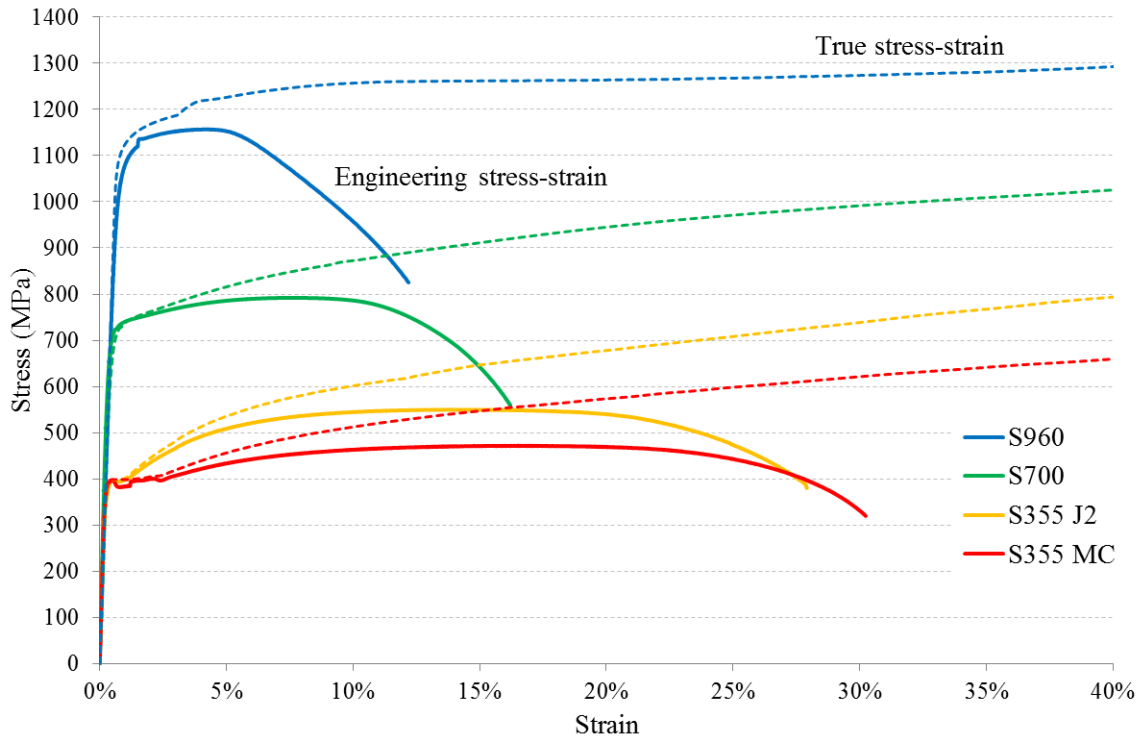


Figure 19. Material stress-strain -curves of the case study. The true stress-strain curves correspond to the case that the Abaqus model of the tension test specimen results to measured engineering curve (Hradil & Talja 2015).

In the case of specimens with a small hole, the maximum equivalent plastic strain at fracture can be somewhat lower than given in Table 3. For example in CHT (centre-hole tension) tests for the materials S960 the calculated maximum strains at experimental failure elongation were 87% for 8 mm hole in flat bar of 80x8 mm². Based on the test results for different notched test specimens, the strains at failure have been found to be always higher than $A5$ (or A_{80}) (Talja & Hradil 2015). Therefore in a common case the failure occurs somewhere between strains of ε_f and $\varepsilon_{eq,f}$. However, because the stress triaxiality at failure of a tension test coupon and CHT specimen are same order of magnitude, $\varepsilon_{eq,f}$ gives a good estimate of the fracture for specimens with a hole.

5.2 Moment-rotation behaviour

M- ϕ curves and plastic axial strains (PE11) in the middle of the tension flange are shown in Figure 20. Axial strains PE11 are taken from distance of 0 mm and 250 mm from the hole. The strains show that when $\varepsilon_{eq,f}$ (Table 3) is reached in specimens with holes, PE11 at 0 mm starts to grow very fast, PE11 at 250 mm strains continues steady growth. The local deformations and reduction of tension area of the cross-section are starting at that moment. In the case of specimens without holes ('no hole'), that kind of failure of the tension flange does not occur (Figure 21).

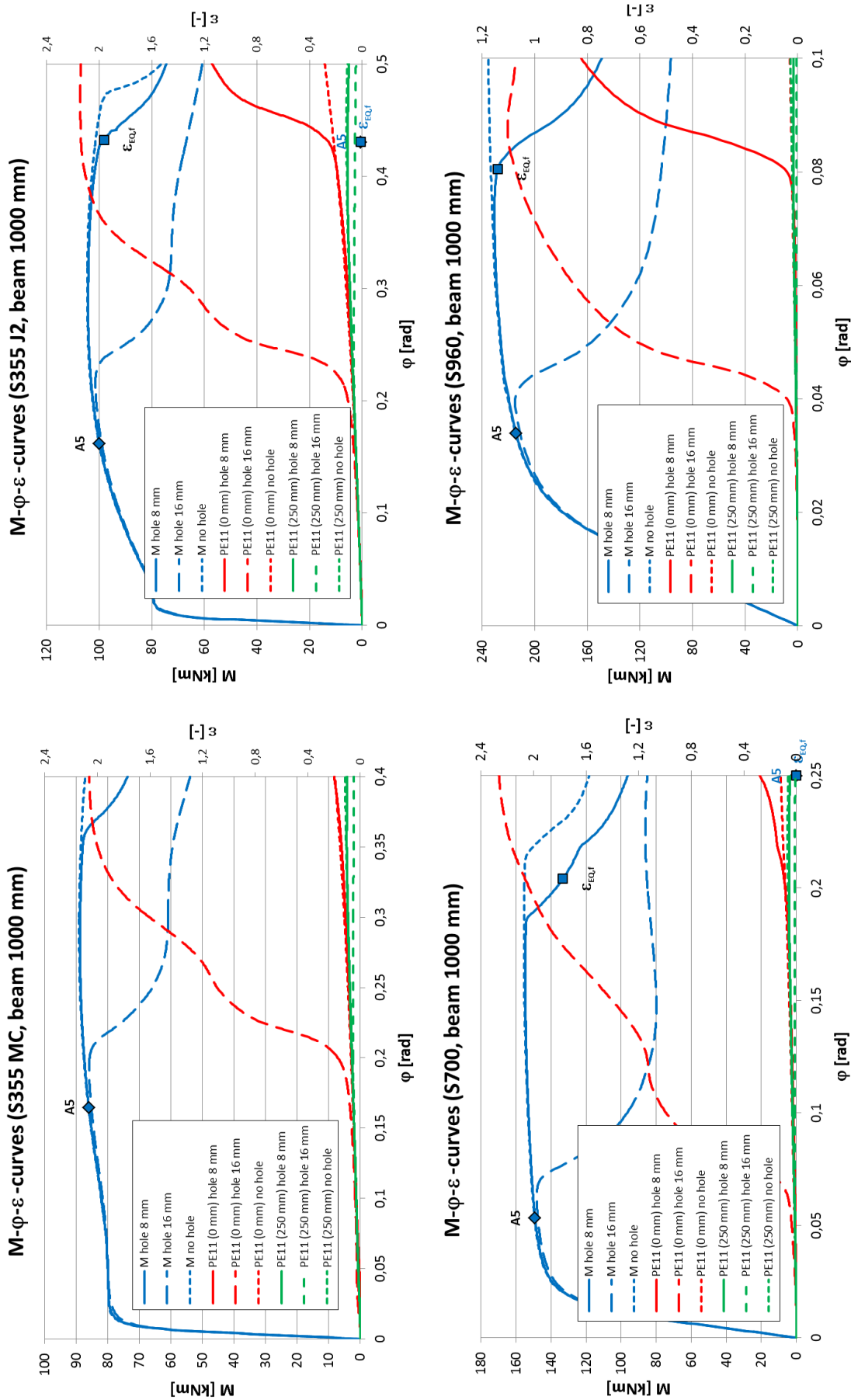
The results assembled in Table 4 show the following:

- In spite of the prevention of plate buckling of the compressed flange, the flange buckles when the rotations are large. In the case of specimens without holes, the flange buckling happens in all cases. The buckling mode resembles beam buckling on elastic foundation (Figure 22).

- ϕ at M_{max} is always less than ϕ at $\varepsilon_{eq,f}$ given in Table 3 (i.e. the maximum load is reached before the strains begin to grow very fast in hole-affected zone). Highest values of elongations ε_{eq} at M_{max} occur in the case of the larger hole.
- The lower is f_u/f_y ratio or ε_u , the lower are the rotations corresponding A5 and $\varepsilon_{eq,f}$.
- The lowest rotations corresponding A5 and $\varepsilon_{eq,f}$ elongations correspond to the biggest hole.
- The rotation corresponding maximum moment is strongly depending of the hole size in the case of S700 and S960 steels.

Table 4. End rotation ϕ (radians) corresponding A5 and $\varepsilon_{eq,f}$ and M_{max} (from Figure 20).

	S355 J2			S355 MC			S700			S960		
f_u / f_y	1.40			1.19			1.12			1.10		
ε_u	13.4%			17.6%			9.5%			3.0%		
Hole	no	8	16	no	8	16	no	8	16	no	8	16
ϕ at flange buckling	0.48	0.46	0.29	>0.40	0.37	0.26	0.22	0.19	-	0.13	-	-
ϕ at $\varepsilon_{eq,max} = A5$	>0.48	>0.16	0.10	>0.40	0.17	0.06	>0.22	0.05	0.03	>0.13	0.03	0.02
ϕ at $\varepsilon_{eq,f}$	>0.48	0.43	0.24	>0.40	>0.37	0.21	>0.22	>0.19	0.07	>0.13	0.08	0.04
ϕ at M_{max}	0.29	0.28	0.22	0.29	0.28	0.19	0.18	0.16	0.05	0.11	0.07	0.04
ε_{eq} at M_{max}	12%	55%	97%	12%	58%	95%	6,7%	70%	74%	3,5%	60%	51%


 Figure 20. M - ϕ curves and plastic strains in tension flange.

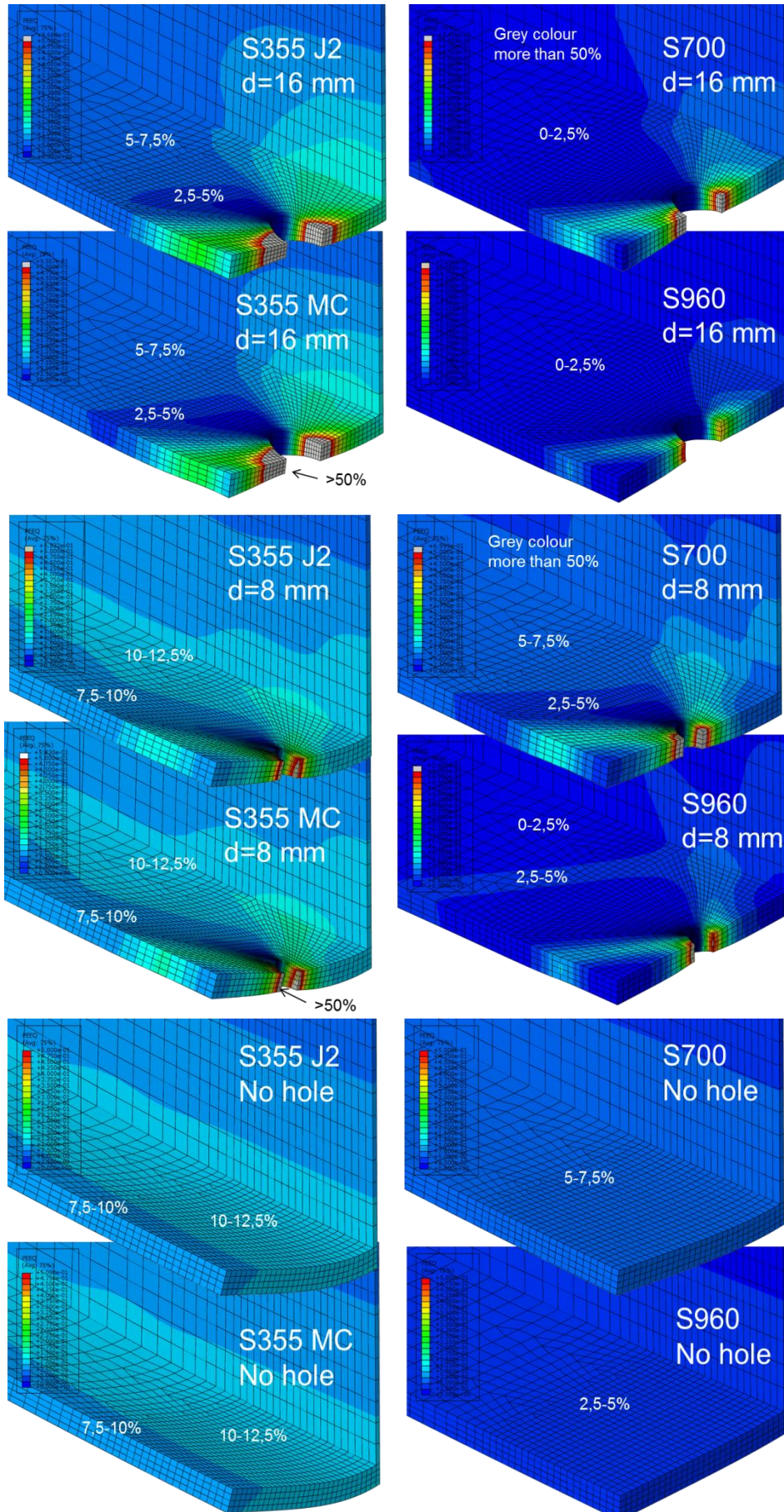


Figure 21. Equivalent plastic strains ε_{eq} when the maximum moment M_{max} is reached (deformations in true scale).

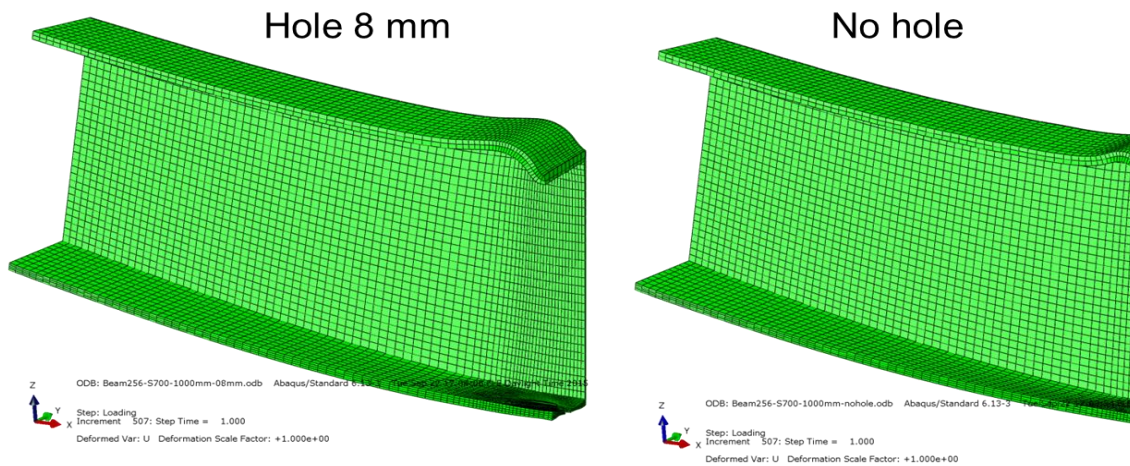


Figure 22. An example of an observed buckling mode of the compression flange (S700).

5.3 Rotation capacity

The moment-rotation relationship $M/M_{pl} - \varphi_{fem}/\varphi_{pl}$ was determined from the results.

The rotation capacity R is calculated from equation

$$R = \frac{\varphi_{fem}}{\varphi_{pl}} - 1, \text{ where } \varphi_{pl} = \frac{M_{pl}L}{EI} \text{ and } M_{pl} = f_y W_{pl} \text{ (Figure 23)}$$

values of I and W_{pl} are based on full gross section. Therefore can be presented (Figure 24)

$$\frac{\varphi_{fem}}{\varphi_{pl}} = R + 1$$

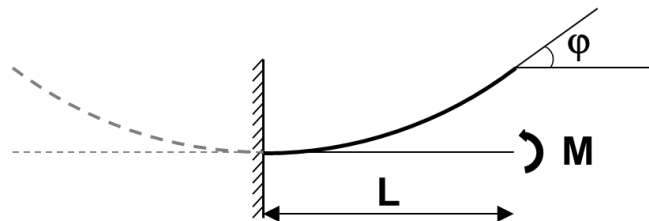


Figure 23. End rotation φ .

Note that the results, presented here, are calculated on the basis of full cross-section properties. If I and W_{pl} would be determined based on net section instead of full cross section, both M_{max}/M_{pl} and $R+1$ would increase by a factor 1.05 (Table 5, hole 8 mm) or 1.10 (hole 16 mm). For the given cross-section $W_{pl}/W = 1.09$.

Table 5. Comparison of net section properties (no hole) to the gross cross section properties with holes 8 and 16 mm.

	no hole	hole 8 mm	hole 16 mm
I	1.0	0.949	0.906
W	1.0	0.922	0.843
W_{pl}	1.0	0.956	0.906

The values concerning rotation capacity R in Table 6 show the following:

- All materials fulfil Eurocode Class 1 requirement $M_{max}/M_{pl} \geq 1.0$, when $\varepsilon_{eq,f}$ failure criterion is used.
- S960 with holes do not fulfil Eurocode Class 1 requirement $M_{max}/M_{pl} \geq 1.0$, if A5 failure criterion is used.
- For specimens without holes $M_{max}/M_{pl} (\varepsilon_{eq,f}) \approx f_u/f_y$, and for S700 and S960 even $> f_u/f_y$
- Except S960 with hole 16 mm, all materials fulfil Eurocode Class 1 requirement $R+1 \geq 4.0$, when $\varepsilon_{eq,f}$ failure criterion is used.
- S355 J2 and S355 MC fulfil Eurocode Class 1 requirement $R+1 \geq 4.0$, even when A5 failure criterion is used.
- $M_{max}/M_{pl} \geq W_{pl}/W_{el} = 1.09$ except S960 with hole 16 mm, when $\varepsilon_{eq,f}$ failure criterion is used.
- M_{max}/M_{pl} and f_u/f_y are the same order of magnitude also for specimen with holes. (When comparing M_{max}/M_{pl} to f_u/f_y , note also that the gross cross section of flange divided by its net cross section is 1.24 for hole 16 mm. For hole 8 mm the ratio is 1.11.)

Table 6. Results of moment-rotation capacity (from Figure 24 and Figure 25).

	S355 J2			S355 MC			S700			S960		
f_u/f_y	1.40			1.19			1.12			1.10		
ε_u	13.4%			17.6%			9.5%			3.0%		
Hole	no	8	16	no	8	16	no	8	16	no	8	16
R at flange buckling	60	58	36	>50	46	32	28	-	24	17	-	-
$M_{max}/M_{pl} (\varepsilon_{eq,f})$	1.39	1.38	1.35	1.17	1.17	1.13	1.15	1.14	1.09	1.16	1.13	1.06
$M_{max}/M_{pl} (A5)$	1.39	1.33	1.22	1.17	1.14	1.06	1.15	1.10	1.04	1.16	1.05	0.96
$R+1 (\varepsilon_{eq,f})$	>60	>58	30	>50	>46	26	15	14	5.0	6.1	3.7	2.0
$R+1 (A5)$	>60	20	12	>50	21	7.3	15	3.7	2.0	6.1	1.6	1.1
$PE11 (250)/\varepsilon_y$	49	47	33	48	47	29	17	15	3,3	5,4	3,0	0,90
$PE11 (max)/\varepsilon_y$	61	78	82	61	54	68	20	38	25	5,7	15	7,3
$PE11 (250)$	9.2%	8.8%	6.2%	9.1%	8.9%	5.5%	5.7%	5.1%	1.1%	2.7%	1.5%	0.5%
$PE11 (max)$	11%	15%	15%	12%	10%	13%	6.7%	13%	8.4%	2.9%	7.6%	3.7%

Figure 25 and Figure 26 show the maximum axial plastic strains in the tension flange at the moment when the maximum value of bending moment is reached. The figure shows the following:

- Except of S960, the hole of 8 mm have no effect on beam behaviour, because the curve of plastic strains for cases ‘no hole’ and ‘hole 8’ have almost equal level. Hole of 16 mm affects in all cases on beam behaviour (Figure 25).
- If the hole has no effect on beam behaviour, plastic strains in the tension flange at the moment when the maximum value of bending moment is reached, are not constant along the beam. It is particularly evident when the value f_u/f_y ratio and ε_u is large (which means that also P11 (250) values are high).
- Except of case ‘no hole’, the maximum axial strain is not located exactly in the middle of beam where the hole locates.

Axial strains in two points of flange are presented in Table 6; $PE11 (max)$ is in the mid-region and $PE11 (250)$ at distance of 250 mm from the hole Plastic strains are also shown relative to $\varepsilon_y = f_y/E$. The table shows the following:

- The lower is f_u/f_y ratio or ε_u , the lower are $PE11 (max)/\varepsilon_y$ and $PE11 (250)/\varepsilon_y$.
- In the case of S355 cases $PE11 (250)/\varepsilon_y = 29\text{--}49$, but for S960 $PE11 (250)/\varepsilon_y = 0.9\text{--}5.4$.
- Except S960 with hole 16 mm, $PE11 (250)/\varepsilon_y \geq 3.0$ (i.e. plastic axial strain in flange outside the hole-affected zone is greater than $3\varepsilon_y$ when M_{max} is reached).
- Except of non-holed S960 beam, $PE11 (250)$ is in all cases less than $\varepsilon_u - f_y/E$.
- In the case of non-holed S960 beam $PE11 (250) = 2.7\% \approx \varepsilon_u - f_y/E = 3.0\% - 0.5\% = 2.5\%$ (i.e. plastic axial strains ε_u of material test are reached in the beam flange). In other cases $PE11 (250) < \varepsilon_u - f_y/E$. Note that if axial strains in flange can reach ε_u , $R = 3$ may be reached in the case of a non-holed beam if $\varepsilon_u \geq 4f_y/E$ (i.e. for S960 $\varepsilon_u \geq 1.9\%$).

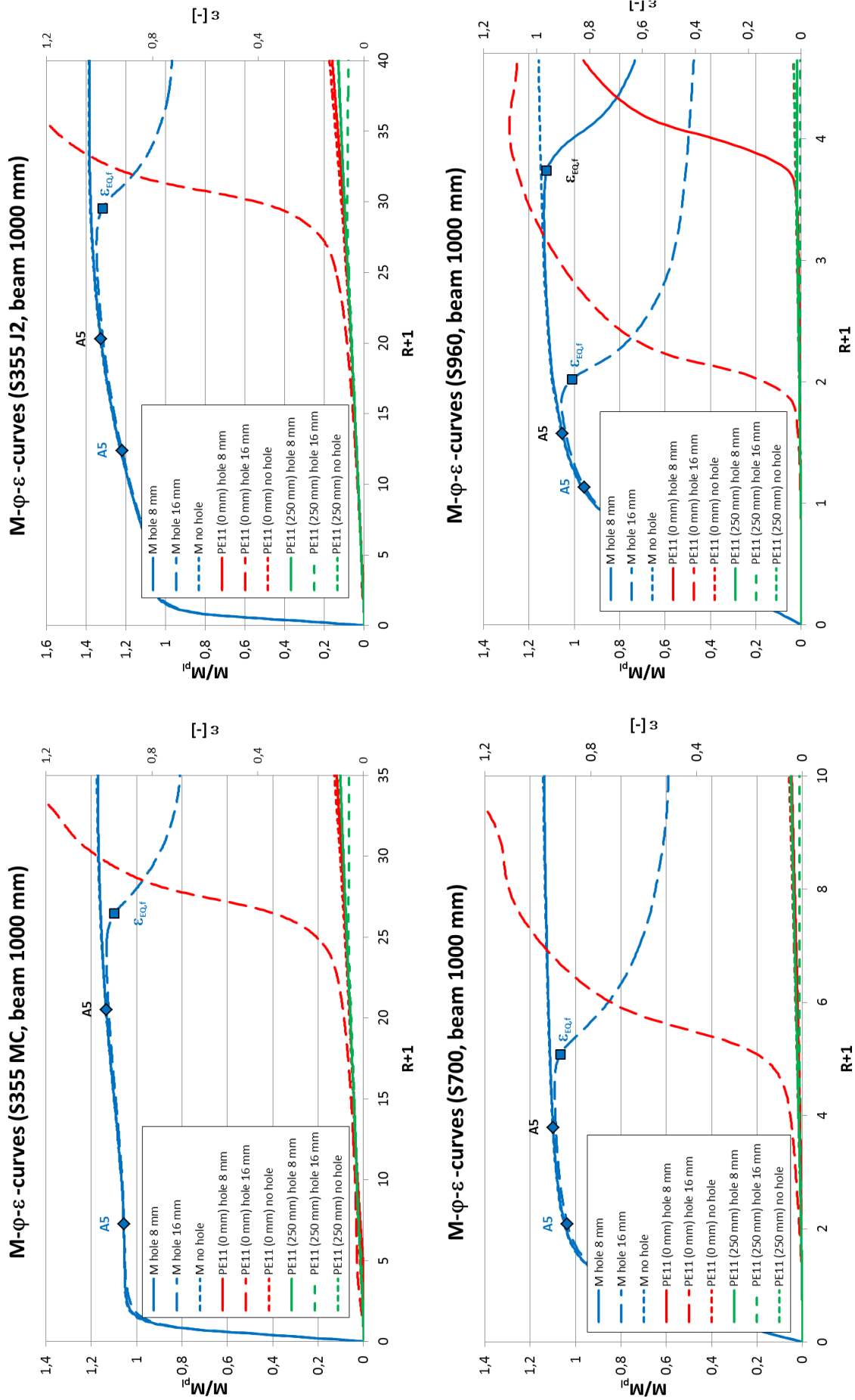


Figure 24. M-R curves and plastic strains in tension flange.

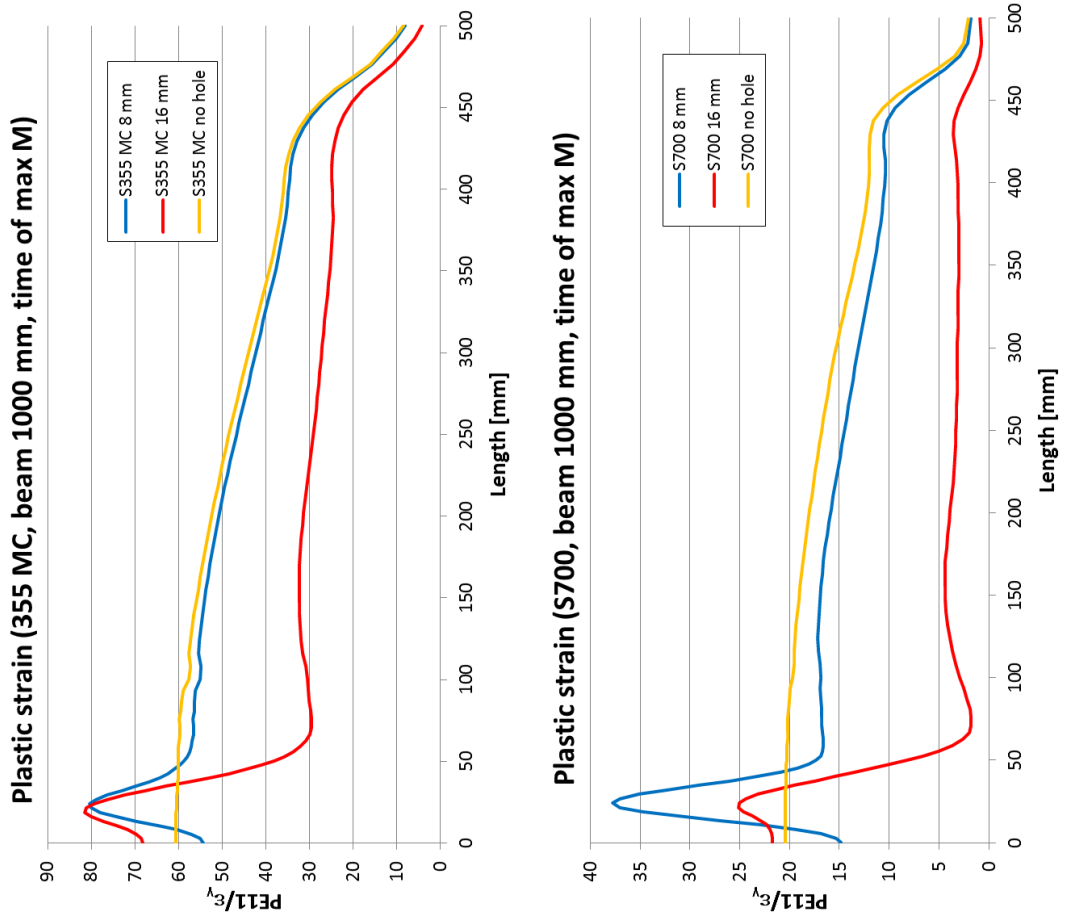
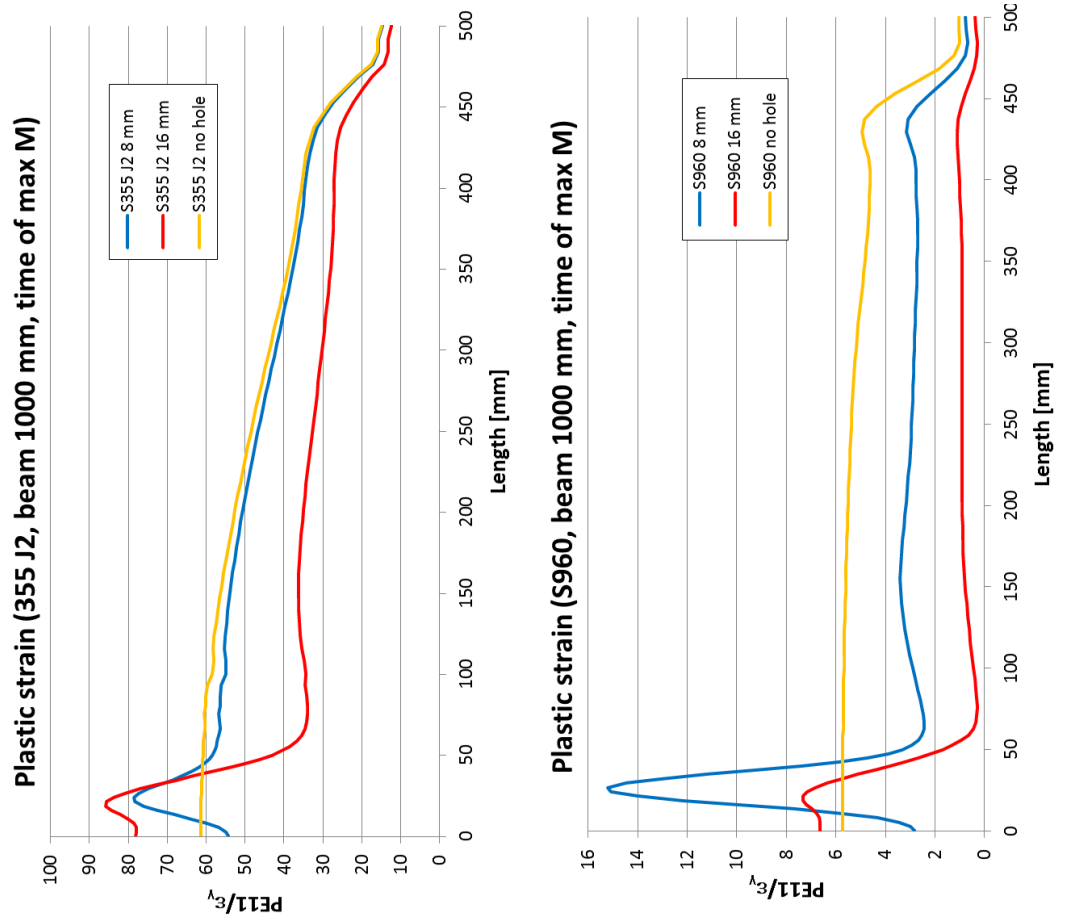


Figure 25. Plastic axial strains along the beam flange.

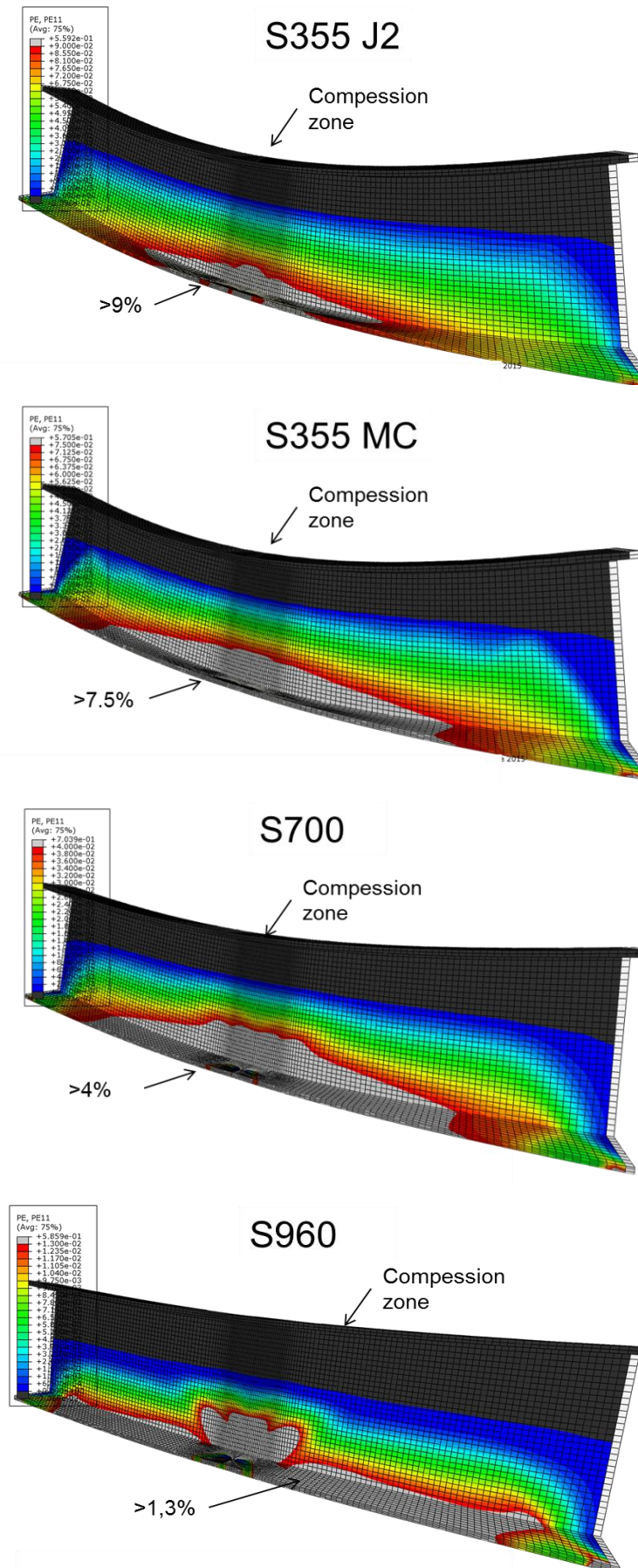


Figure 26. Plastic axial strains ε_{eq} (PE11) for the case of 8 mm hole, at the moment when maximum moment M_{max} is reached (deformations in true scale).

5.4 Effect of beam length on the rotation capacity

To compare the effect of beam length on rotation capacity, the rotation is determined from two different distances from the mid-beam. The rotation capacity R based on the rotation at the distance 250 mm is compared to the value based on rotation at the distance 500 mm (end rotation). Figure 27 shows that the localized plastification at the hole has some effect on R , as described in Section 3.3. The longer the beam, the lower is R . Therefore a relative long beam with half-beam length of $L = 500$ mm is used in this study.

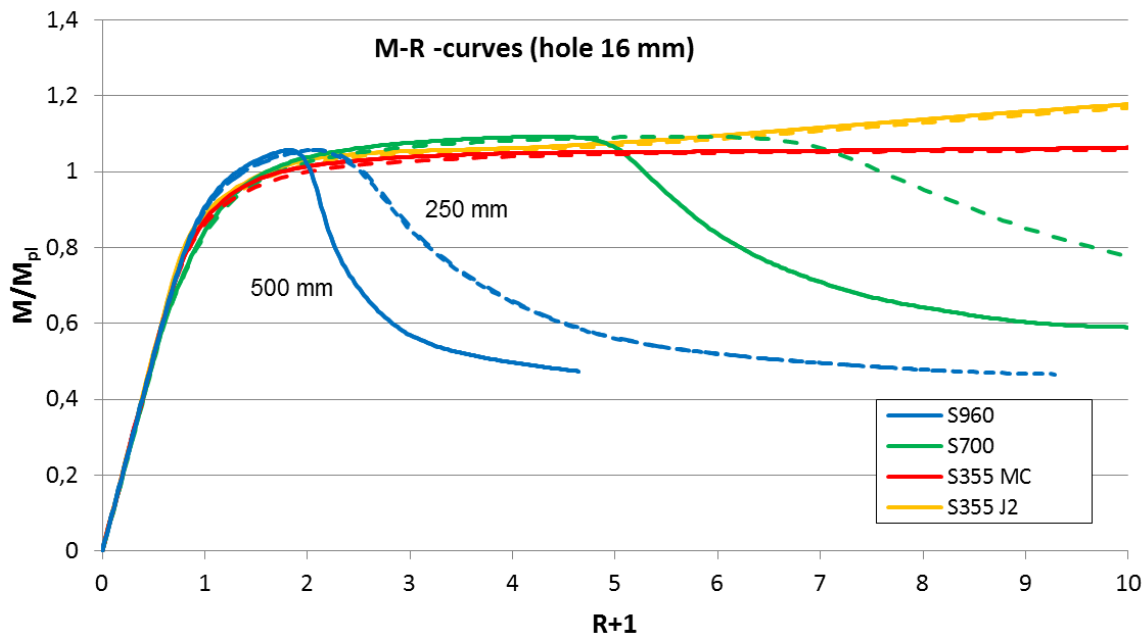


Figure 27. Effect of beam length on rotation capacity R in the case of 16 mm hole.

6. I beam with virtual material properties

The case study is made to see the influence of material properties on Eurocode Class 1 requirement $R \geq 3.0$ and $M_{max}/M_{pl} \geq 1.0$. The comparison is made for the same beam as in previous Section 5.1.

6.1 Material data

Tri-linear material model were used in material modelling (Figure 28). Elastic stage, strain-hardening stage and ideal plastic stage were used for describing true-stress strain curve. This means that strain-hardening was not utilized after the ultimate tensile strength on engineering stress-strain curve was reached.

Eight different material with $f_u/f_y = 1.02-1.2$ and with $\varepsilon_u = 2-10\%$ were under consideration (Table 7). Results with $f_y = 1000$ MPa and $f_y = 500$ MPa were compared. In all cases $E = 210$ GPa was used. Figure 29 compares the new materials to the true stress versus true strain curves of the materials used in previous Section 4.1. SC-10-05 it is most similar to S960.

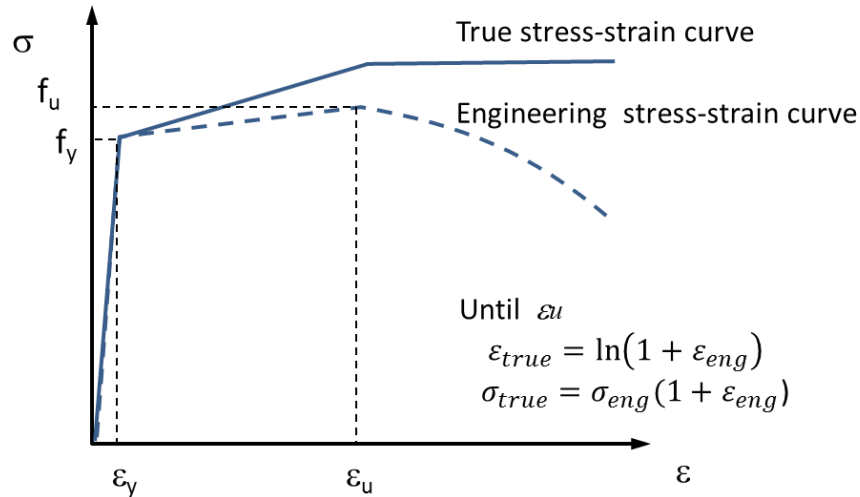


Figure 28. True and engineering stress-strain curves.

Table 7. Material properties for virtual materials.

	Engineering values		True values		Eng. values
	f_u/f_y	ϵ_u	f_u/f_y	ϵ_u	ϵ_u/ϵ_y
SC-02-02	1.02	2%	1.04	2.0%	3.2
SC-02-05	1.02	5%	1.07	4.9%	11
SC-05-02	1.05	2%	1.07	2.0%	3.2
SC-05-05	1.05	5%	1.10	4.9%	11
SC-05-10	1.05	10%	1.16	9.5%	21
SC-10-05	1.10	5%	1.16	4.9%	11
SC-10-10	1.10	10%	1.21	9.5%	21
SC-20-10	1.20	10%	1.32	9.5%	21

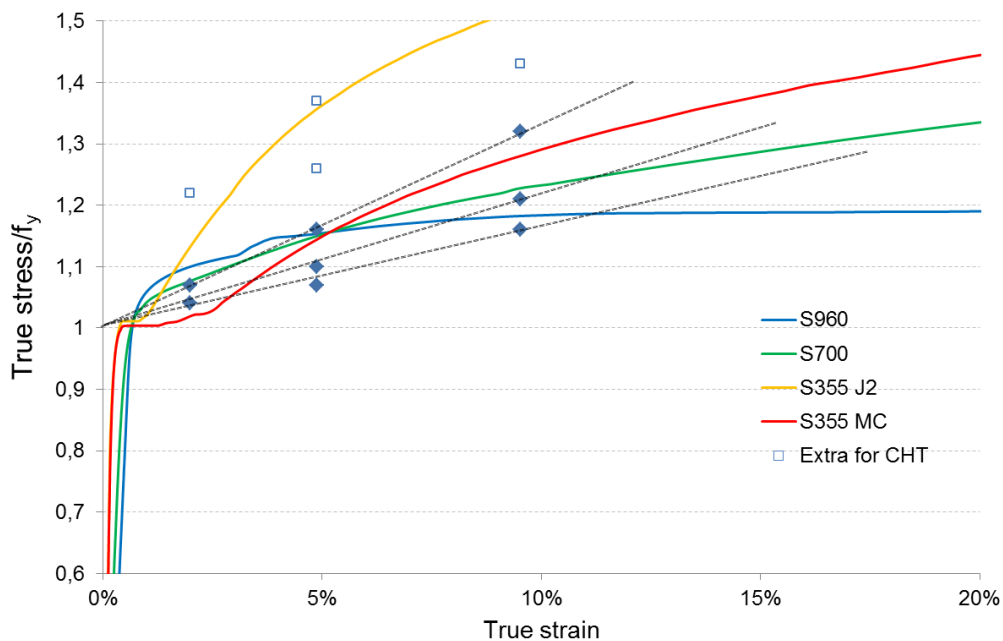


Figure 29. Comparison of virtual and true material models. The dots show the end of strain-hardening stage. The continuous lines show the stress-strain curves of the true materials used in Section 4.1. Open dots are used only for tension plates in section 7.

6.2 Moment-rotation behaviour

Figure 30 and Figure 31 show that in all cases without hole in specimen, and also in some cases with small hole, the failure mode is buckling of the compression flange. However, Figure 32 and Figure 33 show that the maximum bending moment of specimens with hole is reached before the failure starts at the compression flange.

Table 8 and Figure 34 show that when M_{pl} is based on gross cross section, all materials except of SC-02-02 (S1000 and S500) and SC-02-05 (S1000) with hole of 16 mm, fulfil Eurocode Class 1 requirement $M_{max}/M_{pl} \geq 1.0$. However, if $f_u/f_y > W_{pl}/W_{pl,net}$, all cases satisfy the condition $M_{max}/M_{pl} \geq 1.0$. If net section resistance is calculated by $M_u = W_{pl,net} \cdot f_u$, $M_{max}/M_u \geq 1.0$ except of two cases of S1000 with $f_u/f_y = 1.2$, where $M_{max}/M_{pl} = 0.99$ (Figure 34). Comparisons in Figure 34 show also that, besides of hole size, moment resistance M_{max} is affected by the ratio f_u/f_y . The results for case 'no hole' are affected by plate buckling of the compression flange.

Table 8. Ratio of M_{max}/M_{pl} and M_{max}/M_u . Materials with $f_y = 1000$ MPa.

	M_{max}/M_{pl}			M_{max}/M_u		
	hole 16 mm	hole 8 mm	no hole	hole 16 mm	hole 8 mm	no hole
SC-20-10	1.03	1.08*	1.08*	1.04	1.06*	1.05*
SC-10-10	1.01	1.06*	1.06*	1.02	1.05*	1.04*
SC-10-05	1.00	1.06	1.08*	1.03	1.04	1.03*
SC-05-10	0.98	1.04*	1.06*	0.99	0.99*	0.95*
SC-05-05	1.08	1.14	1.14*	1.06	1.07	1.04*
SC-05-02	1.03	1.09	1.13*	1.05	1.06	1.03*
SC-02-05	0.98	1.06*	1.09*	1.06	1.06*	1.01*
SC-02-02	0.96	1.04*	1.07*	1.03	1.03*	0.98*

Table 9. Ratio of M_{max}/M_{pl} and M_{max}/M_u . Materials with $f_y = 500$ MPa.

	M_{max}/M_{pl}			M_{max}/M_u		
	hole 16 mm	hole 8 mm	no hole	hole 16 mm	hole 8 mm	no hole
SC-20-10	1.04	1.09*	1.11*	1.07	1.07*	1.04*
SC-10-10	1.02	1.07*	1.08*	1.06	1.06*	1.05
SC-10-05	1.02	1.07*	1.09*	1.04	1.05*	1.04*
SC-05-10	1.00	1.05*	1.07*	1.00	1.01*	0.99*
SC-05-05	1.09	1.16*	1.19*	1.08	1.08*	1.05*
SC-05-02	1.04	1.10*	1.14*	1.07	1.07*	1.04*
SC-02-05	1.01	1.07*	1.10*	1.08	1.07*	1.03*
SC-02-02	0.99	1.05*	1.07*	1.04	1.04*	1.01*

* Failure starts in compression flange.

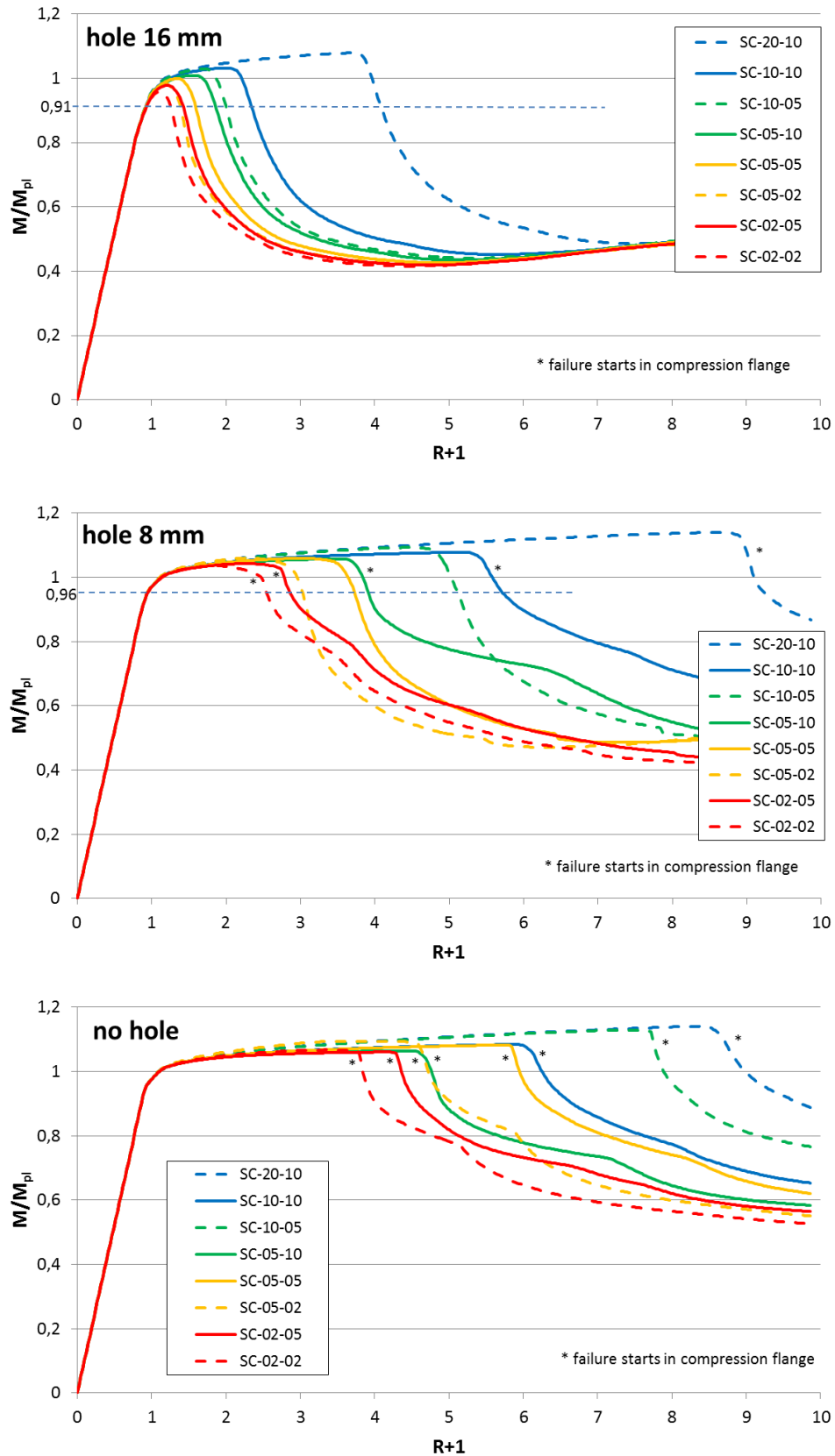


Figure 30. M - R curves of I beams, materials with $f_y = 1000$ MPa.

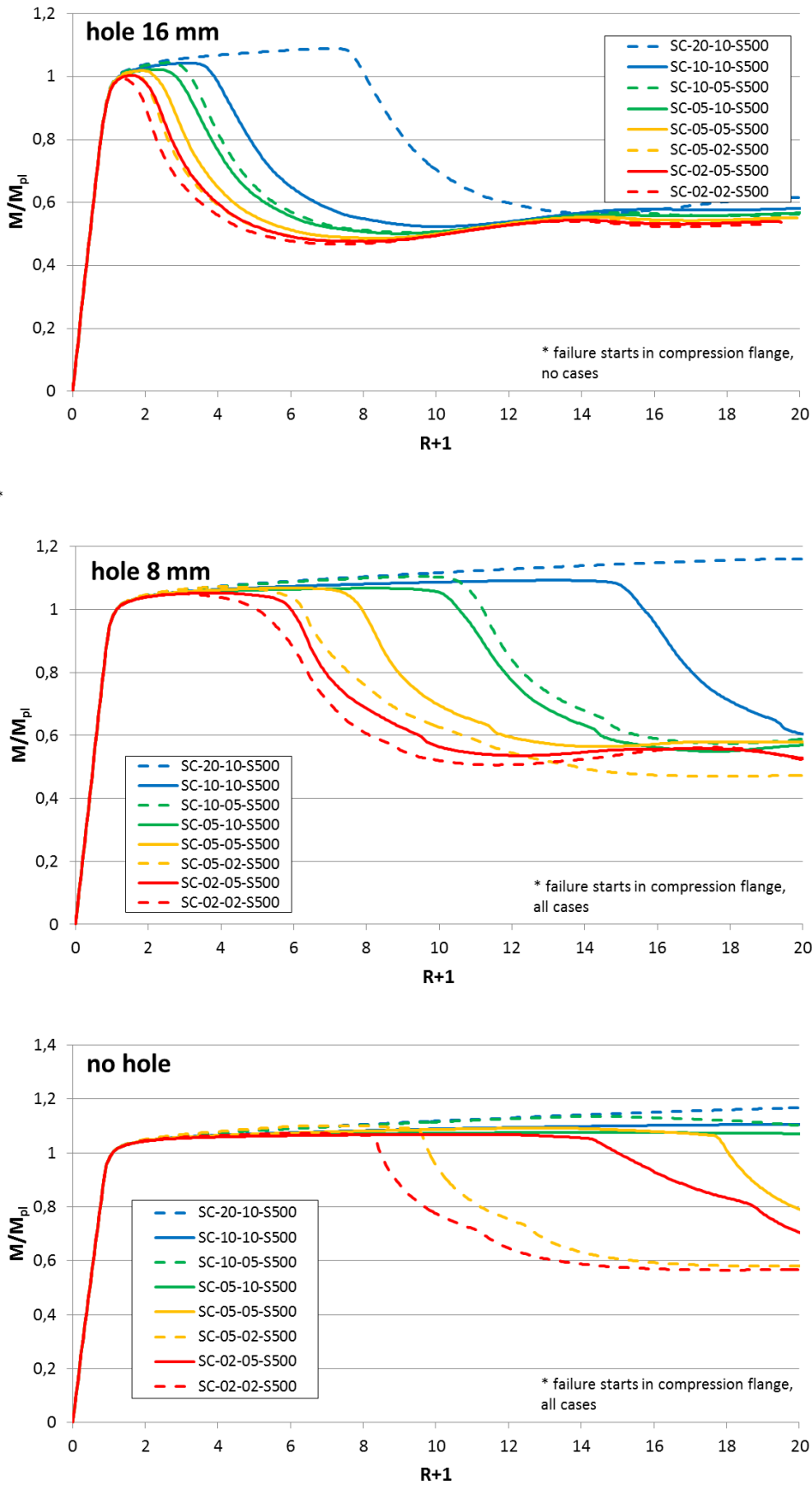


Figure 31. M - R curves of I beams, materials with $f_y = 500$ MPa.

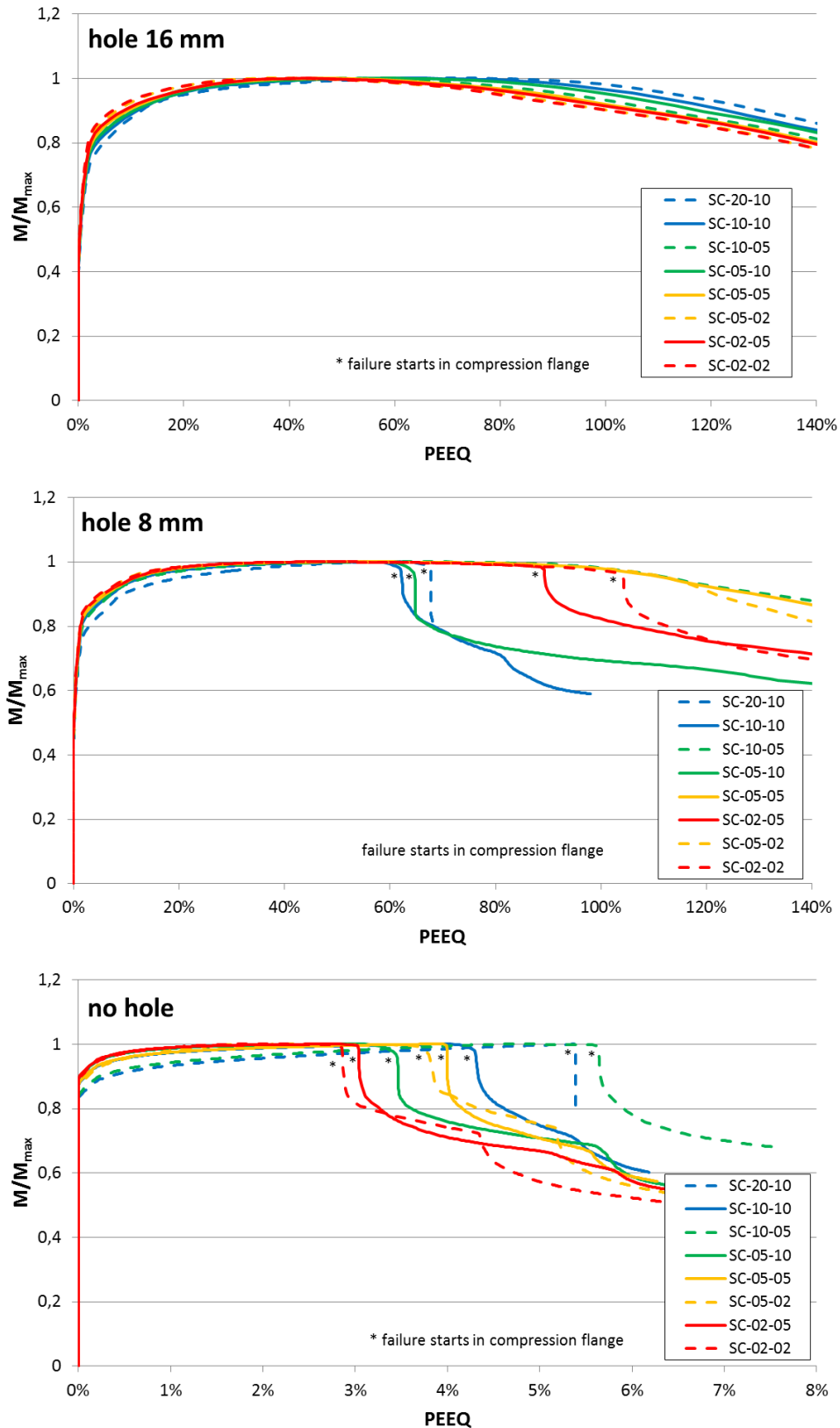


Figure 32. M vs. equivalent plastic strain (PEEQ), materials with $f_y = 1000$ MPa.

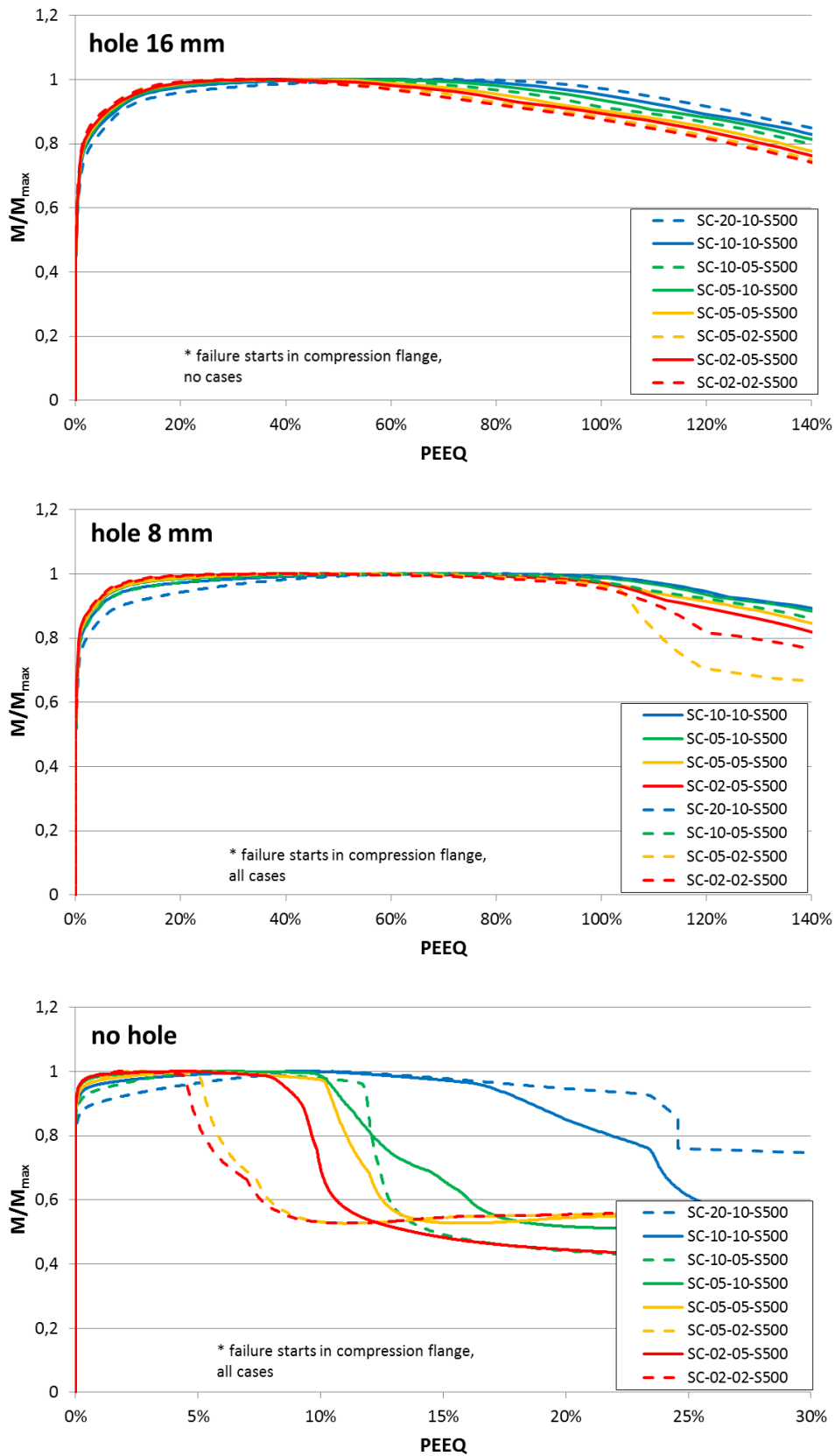


Figure 33. M vs. equivalent plastic strain (PEEQ), materials with $f_y = 500$ MPa.

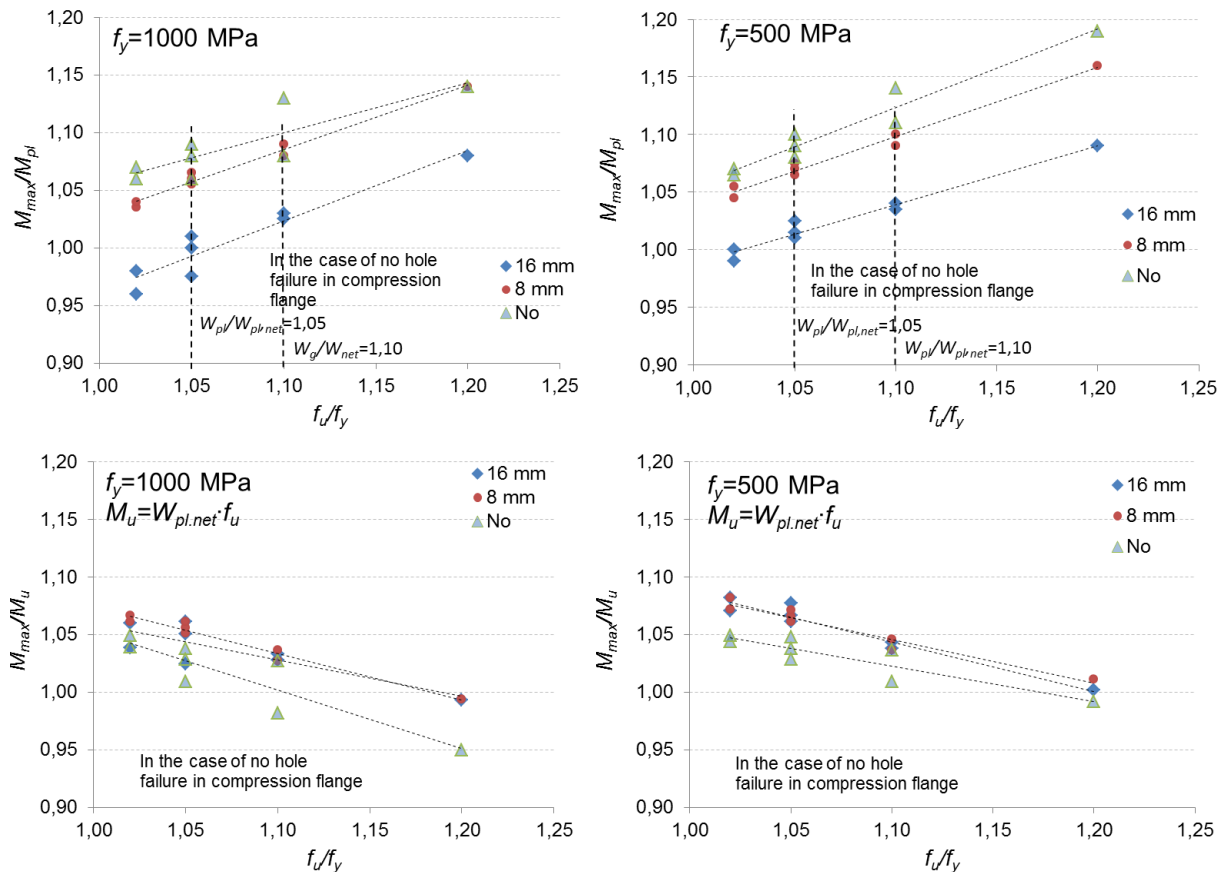


Figure 34. Ratio of M_{max}/M_{pl} and M_{max}/M_u . Materials with $f_y = 1000$ MPa and $f_y = 500$ MPa. The vertical dashed lines show the lower limit of condition $f_u/f_y \geq W_{pl}/W_{pl,net}$ for holes 8 mm and 16 mm (see Table 5).

Table 10, Figure 32 and Figure 33 show that the equivalent plastic strain at the hole is 40–72% for S1000 and 29–77% for S500 when the maximum bending moment is reached and that the strains do not depend much on the size of the hole. The material has to tolerate these plastic strains in order that the conclusions presented here are valid.

Table 10. Equivalent plastic strain (PEEQ) at maximum moment.

	$f_y = 1000$ MPa			$f_y = 500$ MPa		
	hole 16 mm	hole 8 mm	no hole	hole 16 mm	hole 8 mm	no hole
SC-20-10	64%	56%*	3.9%*	59%	69%*	9.2%*
SC-10-10	57%	55%*	3.0%*	49%	61%*	5.6%*
SC-10-05	48%	54%	3.9%*	39%	55%*	4.8%*
SC-05-10	43%	49%*	2.7%*	36%	44%*	4.6%*
SC-05-05	72%	60%	5.4%*	69%	77%*	10%*
SC-05-02	53%	65%	4.7%*	48%	64%*	5.0%*
SC-02-05	40%	49%*	2.5%*	31%	45%*	2.4%*
SC-02-02	42%	47%*	2.0%*	29%	38%*	1.9%*

* Failure starts in compression flange.

Figure 32 and Figure 33 show that the strains begin to grow very fast in hole-affected zone when the maximum load is reached. Therefore, here the rotation capacity R is determined by the maximum point of the moment-rotation curve. This is a conservative assumption, because the descending part of the curve is not utilized.

Figure 35 shows that rotation capacity $R = 3$ is reached in this case study, if calculated $M_{max} = 1.06-1.09 \cdot M_{pl}$. Therefore the correct estimation of the design value for M_{max} is very important.

Figure 36 shows that the $R < 3$ values are more dominant in the case of hole 16 mm than in the case of 8 mm. Ratio of $f_u/f_y = 1.1 \cdot W_{pl}/W_{pl,net}$, with values of 1.15 and 1.21 for holes 8 mm and 16 mm, seems to be a conservative estimate for $R \geq 3$. Figure 36 shows also that R is slightly depending on ε_u and f_u/f_y ratio.

The theoretical value for the rotation capacity of the beam without holes in this study ($W_{pl}/W = 1.09$) is

$$R_u = \frac{W}{W_{pl}} \frac{\varepsilon_u}{\varepsilon_y} - 1$$

The equation is based on beams without holes and assumption that $\varepsilon_{max} = \varepsilon_u$ (see Chapter 2.1). When $\varepsilon_u = 2\%$, $R_u = 2.9$ for S1000 and $R_u = 6.7$ for S500 ($E = 210$ GPa). These R_u values are not exactly reached in the case materials SC-05-02 and SC-02-2 and (Table 11, no hole). However, it has to be noted that the rotation capacities of the beams without hole were limited by the plate buckling of the compression flange.

Table 11. Moment-rotation capacity R .

	$f_y = 1000$ MPa			$f_y = 500$ MPa		
	hole 16 mm	hole 8 mm	no hole	hole 16 mm	hole 8 mm	no hole
SC-20-10	2.7	7.7*	7.4*	6.2	19*	25*
SC-10-10	1.0	4.2*	4.9*	2.2	12*	21*
SC-10-05	0.7	3.5	6.3*	1.7	8.4*	13*
SC-05-10	0.5	2.5*	3.0*	1.3	7.1*	13*
SC-05-05	0.4	2.0	4.8*	0.9	4.9*	12*
SC-05-02	0.2	1.3	3.0*	0.6	3.1*	6.2*
SC-02-05	0.2	1.3*	3.2*	0.6	2.7*	10*
SC-02-02	0.1	0.8*	2.6*	0.4	1.9*	4.9*

* Failure starts in compression flange.

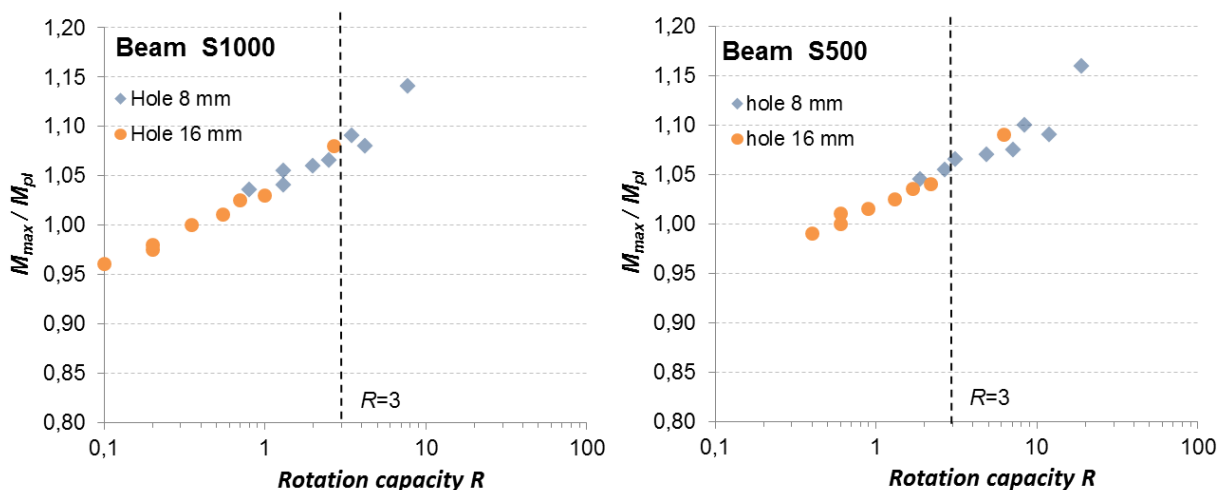


Figure 35. Comparison of M_{max}/M_{pl} to rotation capacity R . The plots are based on results in Table 8, Table 9 and Table 11.

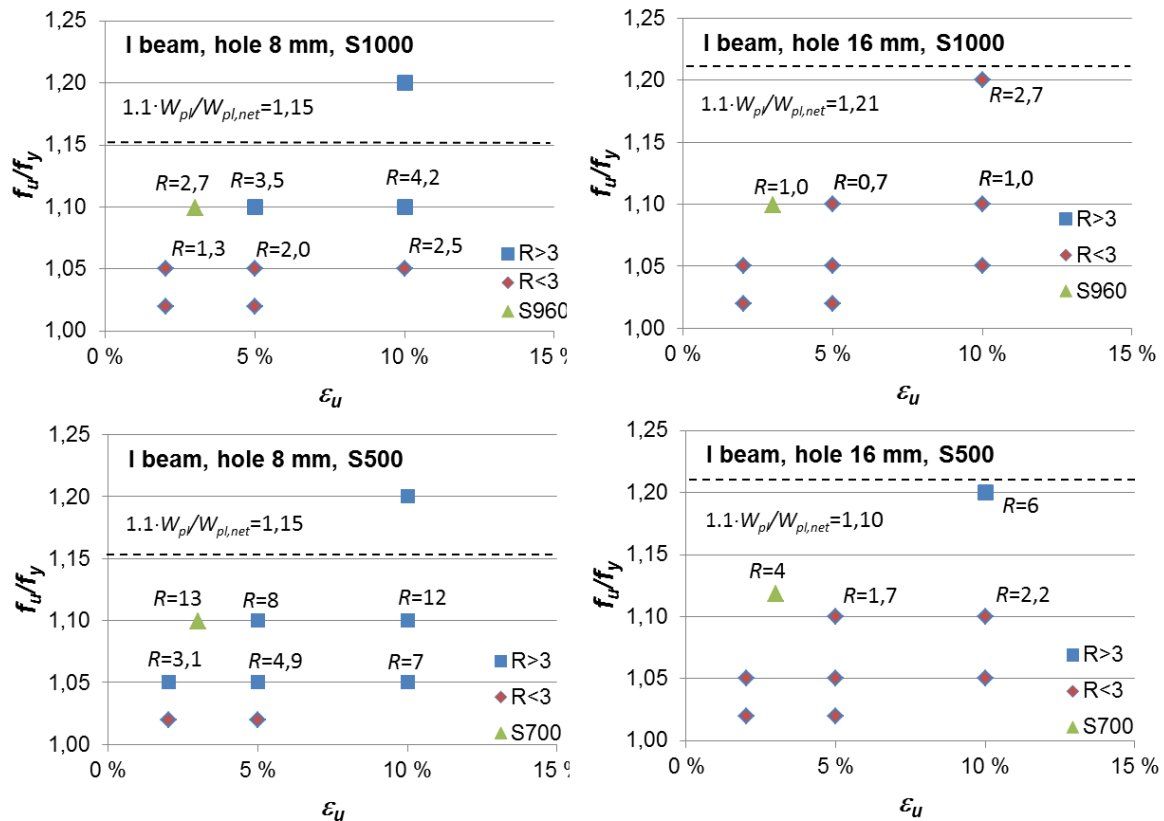


Figure 36. Material models which results to moment-rotation capacities of $R > 3$ and $R < 3$. The horizontal dashed lines show the values of $1.1 \cdot W_p/W_{pl,net}$.

7. Centre hole tension specimens with virtual material properties

7.1 Material data

A flat bar with length of 1000 mm, width $b = 80$ mm and thickness $t = 8$ mm, having a hole in the middle, is modelled in tension; thus corresponding to half of beam flange in the previous study. The flat bar can be understood as ideal cases of a beam with zero web thickness. One eighth of the flat bar with length of $L = 500$ mm is modelled.

Specimens with hole of 16 mm and 8 mm and bars without hole are modelled. Materials with $f_y = 1000$ MPa and $f_y = 500$ MPa are studied.

In addition of the previous materials use for beams (Table 7), four additional material models SC-20-02, SC-20-05, SC-30-05 and SC-30-10 (Table 12) are used in this case.

Table 12. Material properties of centre hole tension specimens.

	Engineering values		True values	
	f_u/f_y	ϵ_u	f_u/f_y	ϵ_u
SC-02-02	1.02	2%	1.04	2.0%
SC-05-02	1.05	2%	1.07	2.0%
SC-10-05	1.10	5%	1.16	4.9%
SC-20-10	1.20	10%	1.32	9.5%
SC-02-05	1.02	5%	1.07	4.9%
SC-05-05	1.05	5%	1.10	4.9%
SC-05-10	1.05	10%	1.16	9.5%
SC-10-10	1.10	10%	1.21	9.5%
SC-20-02	1.20	2 %	1.22	2.0%
SC-20-05	1.20	5%	1.26	4.9%
SC-30-05	1.30	5%	1.37	4.9%
SC-30-10	1.30	10%	1.43	9.5%

7.2 Force-displacement behaviour

Lengthening capacity R is determined by

$$R_t = \frac{\epsilon_{max}}{\epsilon_y} - 1 = \frac{\Delta_{max}}{\Delta_y} - 1; \quad \Delta_y = L \frac{f_y}{E}$$

It should also be noted that the equation assumes that the geometry and behaviour of the compression flange are identical with those of the tension flange. In addition the web of a beam affects not only the bending resistance. Therefore the results with the tension plate approach are not fully comparable with the results of the beam model.

Plastic tensile resistance is determined by

$$F_{pl} = F_y = A_g \cdot f_y$$

Ultimate tensile resistance is determined by

$$F_u = A_{net} \cdot f_u$$

In addition reduced ultimate tensile resistance $F_{u,r}$ is used in comparisons.

$$F_{u,r} = \frac{A_{net} \cdot f_u}{k}; \quad k_r = 1 + 0.1 \left(\frac{f_u}{f_y} - 1 \right)$$

Table 13, Table 14 and Figure 37 (top graphs) show that in all cases $F_{max}/F_y \geq 1.0$, if $f_u/f_y \geq A_g/A_{net}$. However, when the trend lines in Figure 37 are considered, F_{max}/F_y may be slightly less than 1.0 when $A_g/A_{net} = 1.25$ (hole 16 mm, S500). This means that the condition $f_u/f_y \geq A_g/A_{net}$ can be slightly unsafe.

All cases which have been modelled until the maximum load do not fulfil $F_{max}/F_u \geq 1.0$ (Figure 37, mid graphs). In the case of hole 16 mm and high f_u/f_y ratios F_{max} can be 2–3% less than F_u . However, if small reduction factor k_r (dependant on f_u/f_y) is used for F_u , all results will be conservative (Figure 37, bottom graphs). Results for both S1000 and S500 are almost identical.

Table 15, Table 16 and Figure 42 show that the equivalent plastic strains at the hole are 10–57% for S1000 and 11–53% for S500 when the maximum axial force is reached. The strains do not depend much on the size of the hole.

Figure 38 shows that lengthening capacity $R_t = 3$ is reached, when calculated $F_{max} = 1.01–1.09 \cdot F_{pl}$. Therefore the correct estimation of the design value for F_{max} is very important.

Figure 39 shows that the $R_t < 3$ values are more dominant in the case of hole 16 mm than in the case of 8 mm. Ratio of $f_u/f_y = 1.1 \cdot A_g/A_{net,t}$, with values of 1.22 and 1.38 for holes 8 mm and 16 mm seems to be a conservative estimate for $R \geq 3$. Figure 39 shows also that R is slightly depending on ε_u and f_u/f_y ratio.

The theoretical value for lengthening capacity of flat bars without holes is $R_{t,u} = \varepsilon_u/\varepsilon_y - 1$, when the capacity R_t is determined based on the maximum point of load-displacement curve. In the case of $\varepsilon_u = 2\%$, $R_{t,u} = 3.2$ for S1000 and $R_{t,u} = 7.4$ for S500 ($E = 210$ GPa). For those cases where the maximum elongation has been determined $R_{t,u}$ is quite exactly equal to R_u (Table 15 and Table 16, case 'no hole').

Table 13. Ratio of F_{max}/F_y and F_{max}/F_u . Materials with $f_y = 1000$ MPa.

	F_{max}/F_y			F_{max}/F_u		
	hole 16 mm	hole 8 mm	no hole	hole 16 mm	hole 8 mm	no hole
SC-02-02	0.82	0.93	1.02	1.01	1.01	1.00
SC-05-02	0.84	0.95	1.05	1.00	1.01	1.00
SC-10-05	0.88	0.99	1.08 ¹⁾	1.00	1.00	0.98 ¹⁾
SC-20-10	0.94	1.07	1.10 ²⁾	0.98	0.99	0.92 ²⁾
SC-02-05	0.83	0.93	1.02	1.02	1.01	1.00
SC-05-05	0.84	0.95	1.05 ²⁾	1.00	1.01	1.00 ²⁾
SC-05-10	0.84	0.95	1.02 ²⁾	1.00	1.01	0.97 ²⁾
SC-10-10	0.87	0.99	1.05 ²⁾	0.99	1.00	0.95 ²⁾
SC-20-02	0.96	1.08	1.20	1.00	1.00	1.00
SC-20-05	0.94	1.08	1.19 ²⁾	0.98	1.00	0.99 ²⁾
SC-30-05	1.02	1.17	1.28 ²⁾	0.98	1.00	0.98 ²⁾
SC-30-10	1.01	1.14 ²⁾	1.15 ²⁾	0.97	0.97 ²⁾	0.88 ²⁾

¹⁾ Calculated only up to elongation of 4% ²⁾ Calculated only up to elongation of 5%.

Table 14. Ratio of F_{max}/F_y and F_{max}/F_u . Materials with $f_y = 500$ MPa.

	F_{max}/F_y			F_{max}/F_u		
	hole 16 mm	hole 8 mm	no hole	hole 16 mm	hole 8 mm	no hole
SC-02-02	0.83	0.93	1.02	1.02	1.01	1.00
SC-05-02	0.85	0.96	1.05	1.01	1.02	1.00
SC-10-05	0.88	1.00	1.08 ¹⁾	1.00	1.01 ¹⁾	0.98 ¹⁾
SC-20-10	0.94	1.08	1.10 ²⁾	0.98	1.00 ²⁾	0.92 ²⁾
SC-02-05	0.83	0.94	1.02	1.02	1.02	1.00
SC-05-05	0.85	0.96	1.05 ²⁾	1.01	1.02 ²⁾	1.00 ²⁾
SC-05-10	0.85	0.96	1.03 ²⁾	1.01	1.02 ²⁾	0.98 ²⁾
SC-10-10	0.88	1.00	1.05 ²⁾	1.00	1.01 ²⁾	0.95 ²⁾
SC-20-02	0.96	1.09	1.20	1.00	1.01	1.00
SC-20-05	0.95	1.08	1.20 ²⁾	0.99	1.00 ²⁾	1.00 ²⁾
SC-30-05	1.03	1.17	1.29 ²⁾	0.99	1.00 ²⁾	0.99 ²⁾
SC-30-10	1.01	1.15 ²⁾	1.16 ²⁾	0.97	0.98 ²⁾	0.89 ²⁾

¹⁾ Calculated only up to elongation of 4% ²⁾ Calculated only up to elongation of 5%.

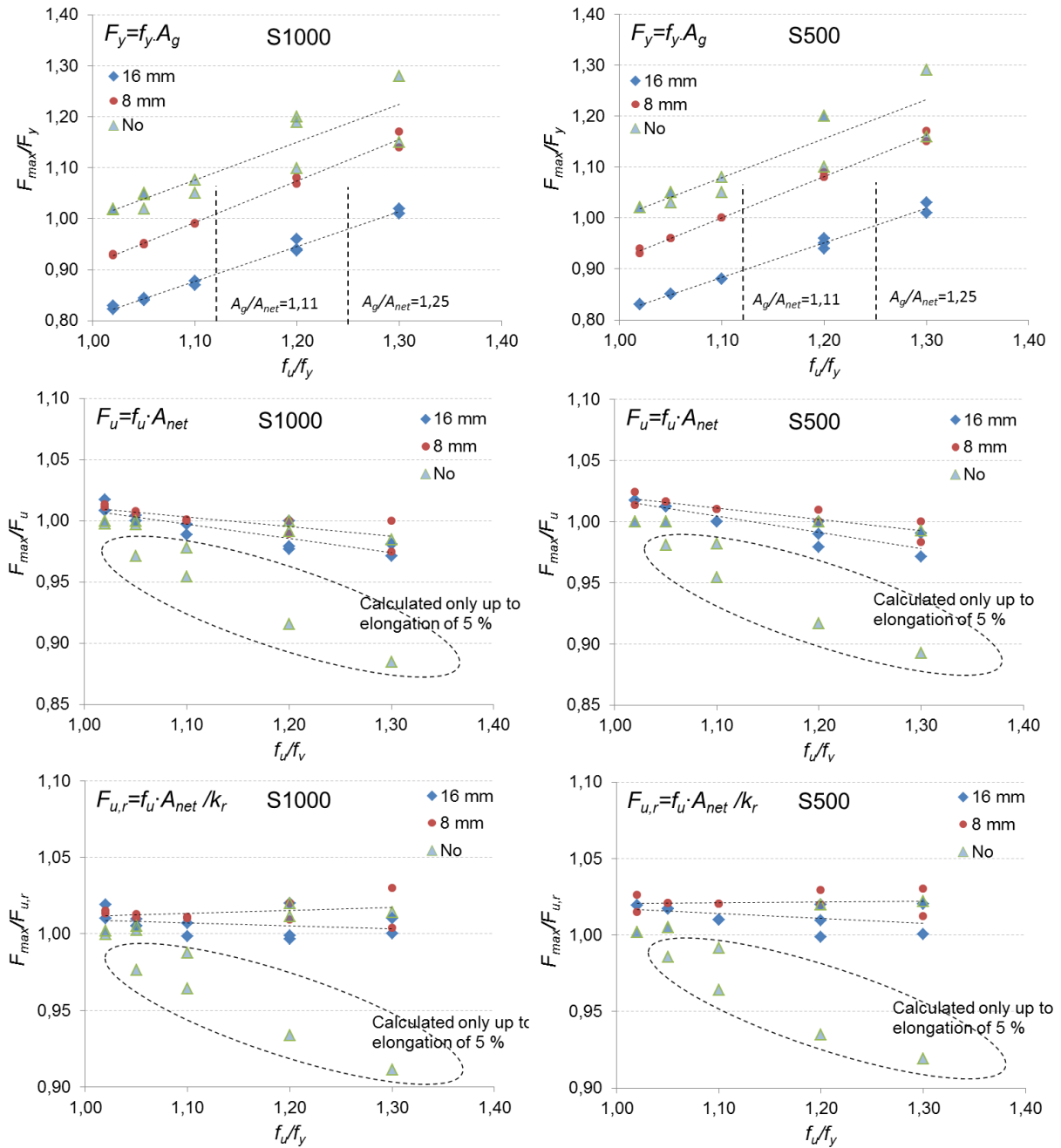


Figure 37. F_{max}/F_y and F_{max}/F_u vs. f_u/f_y for centre hole flat bars. The vertical dashed lines in topmost graphs show the lower limit of condition $f_u/f_y \geq A_g/A_{net}$ for holes 8 mm and 16 mm (see Table 5).

Table 15. Equivalent plastic strain (PEEQ) at maximum force and R_t factors for centre hole flat bars. Materials with $f_y = 1000$ MPa.

	PEEQ			R_t			Note
	hole 16 mm	hole 8 mm	no hole	hole 16 mm	hole 8 mm	no hole	$\varepsilon_u/\varepsilon_y-1$
SC-02-02	10%	11%	1.5%	-0.08	0.02	3.1	3.2
SC-05-02	13%	14%	1.5%	-0.03	0.08	3.2	3.2
SC-10-05	30%	37%	3.5% ¹⁾	0.23	0.39	7.4 ¹⁾	9.5
SC-20-10	52%	57%	4.4% ²⁾	0.68	7.0	9.5 ²⁾	20
SC-02-05	22%	24%	4.5 %	0.05	0.16	9.3	9.5
SC-05-05	27%	31%	4.5 % ²⁾	0.13	0.26	9.5 ²⁾	9.5
SC-05-10	36%	43%	4.5 % ²⁾	0.26	0.42	9.5 ²⁾	20
SC-10-10	43%	49%	4.4 % ²⁾	0.41	0.58	9.5 ²⁾	20
SC-20-02	16%	15%	1.5%	0.16	1.6	3.4	3.2
SC-20-05	35%	37%	4.3% ²⁾	0.42	4.0	9.5 ²⁾	9.5
SC-30-05	40%	34%	4.3% ²⁾	1.3	5.7	9.5 ²⁾	9.5
SC-30-10	56%	41% ²⁾	4.4% ²⁾	1.4	9.5 ²⁾	9.5 ²⁾	20

¹⁾ Calculated only up to elongation of 4% ²⁾ Calculated only up to elongation of 5%.

Table 16. Equivalent plastic strain (PEEQ) at maximum force and R_t factors for centre hole flat bars. Materials with $f_y = 500$ MPa.

	PEEQ			R_t			Note
	hole 16 mm	hole 8 mm	no hole	hole 16 mm	hole 8 mm	no hole	$\varepsilon_u/\varepsilon_y-1$
SC-02-02	11%	12%	1.8%	0.05	0.16	7.2	7.4
SC-05-02	12%	16%	1.8%	0.10	0.26	7.3	7.4
SC-10-05	30%	36%	3.7% ¹⁾	0.63	0.84	15.9 ¹⁾	20
SC-20-10	49%	53%	4.7% ²⁾	1.47	16.3	20.0 ²⁾	41
SC-02-05	23%	24%	4.7%	0.31	0.42	19.4	20
SC-05-05	27%	31%	4.7% ²⁾	0.47	0.63	20.0 ²⁾	20
SC-05-10	35%	43%	4.8% ²⁾	0.73	0.99	20.0 ²⁾	41
SC-10-10	43%	50%	4.7% ²⁾	1.05	1.31	20.0 ²⁾	41
SC-20-02	18%	16%	1.8%	0.42	3.6	7.6	7.4
SC-20-05	35%	33%	4.6% ²⁾	0.79	8.8	20.0 ²⁾	20
SC-30-05	36%	31%	4.6% ²⁾	2.89	12.0	20.0 ²⁾	20
SC-30-10	53%	37% ²⁾	4.6% ²⁾	3.52	20.0 ²⁾	20.0 ²⁾	41

¹⁾ Calculated only up to elongation of 4% ²⁾ Calculated only up to elongation of 5%.

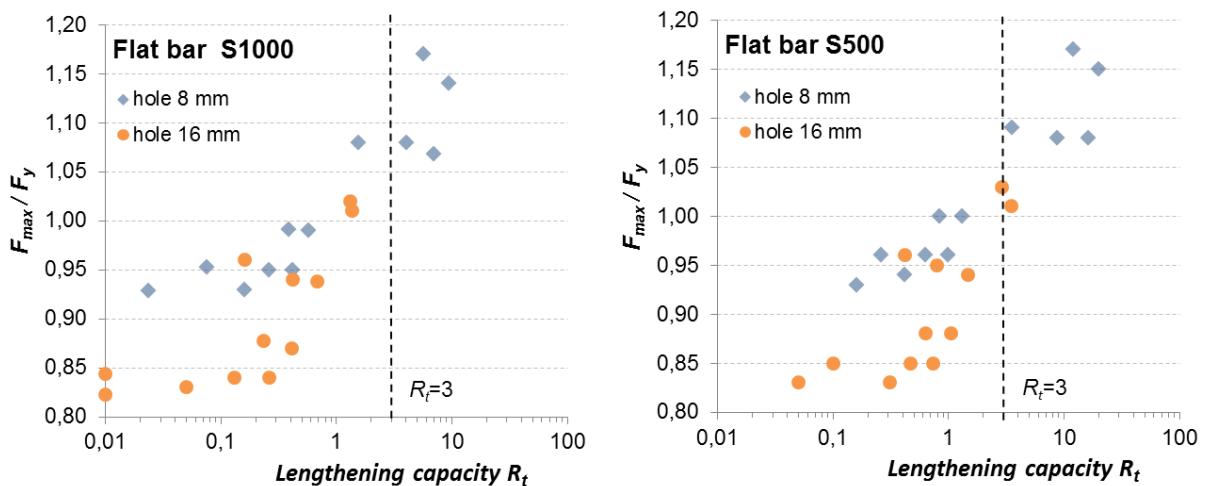


Figure 38. Comparison of F_{max}/F_{pl} to lengthening capacity R_t .

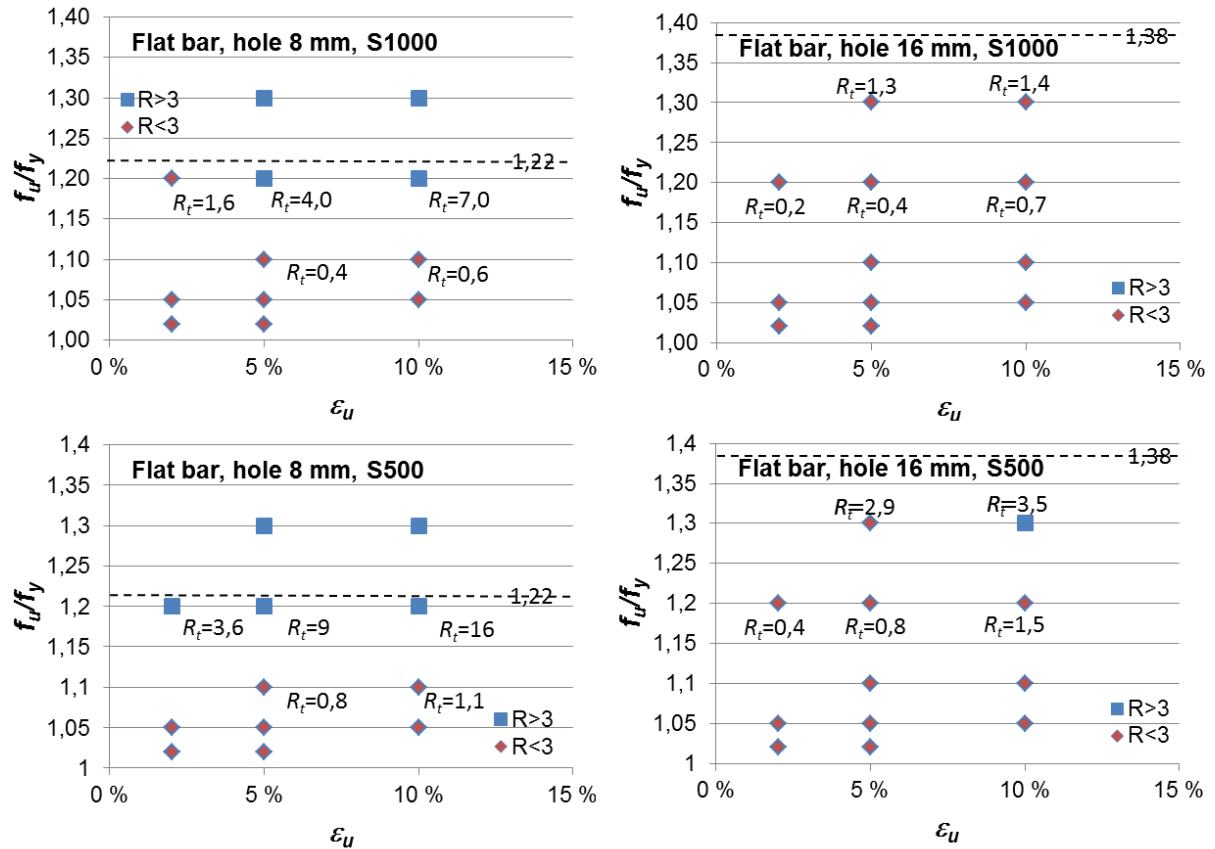


Figure 39. Material models which results to lengthening capacities of $R_t > 3$ and $R_t < 3$. The values on the horizontal dashed lines show the value of $1.1 \cdot A_g/A_{net}$.

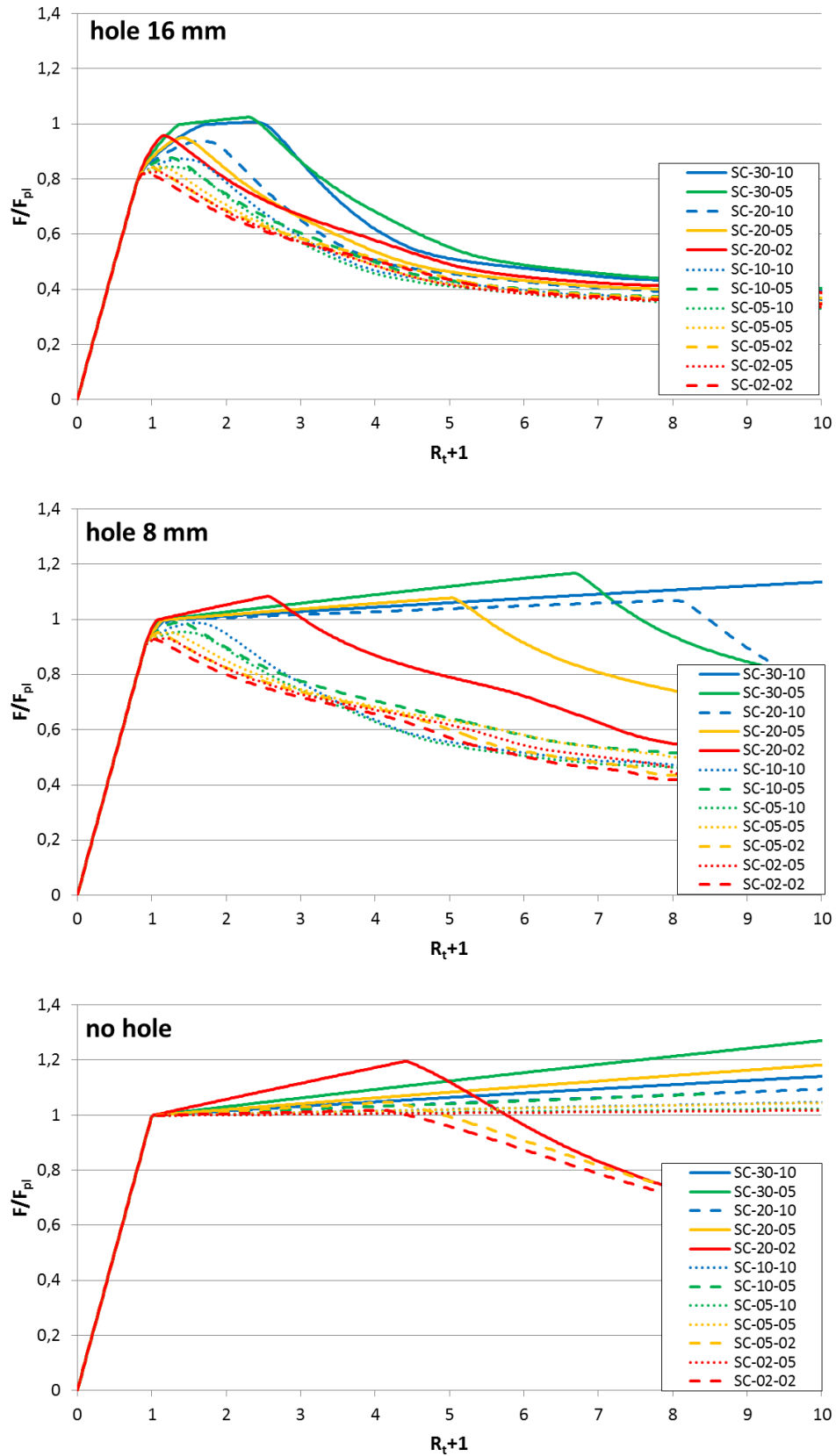


Figure 40. $F-R_t$ curves for centre hole flat bars. Materials with $f_y = 1000$ MPa.

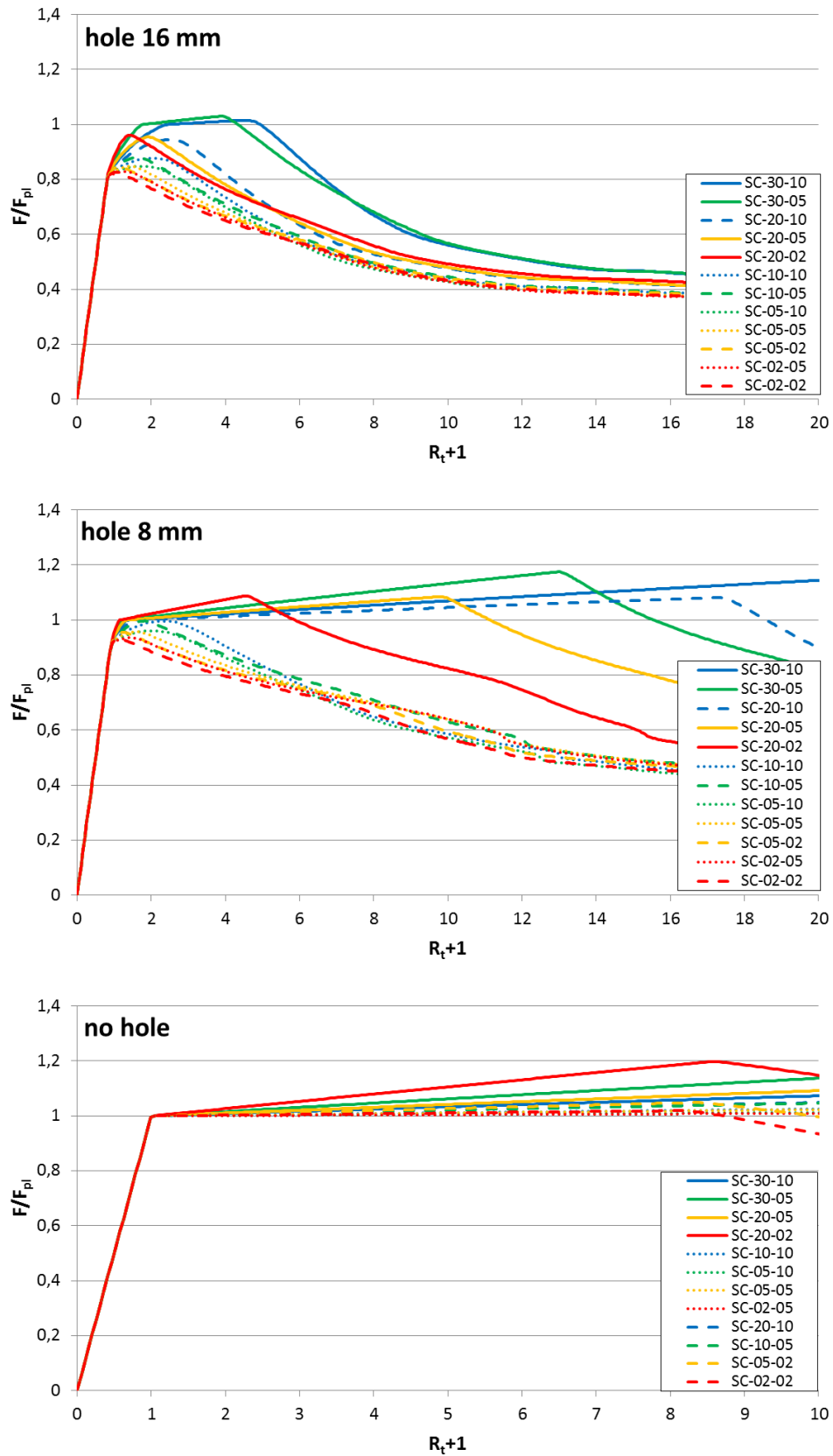


Figure 41. $F-R_t$ curves for centre hole flat bars. Materials with $f_y = 500$ MPa.

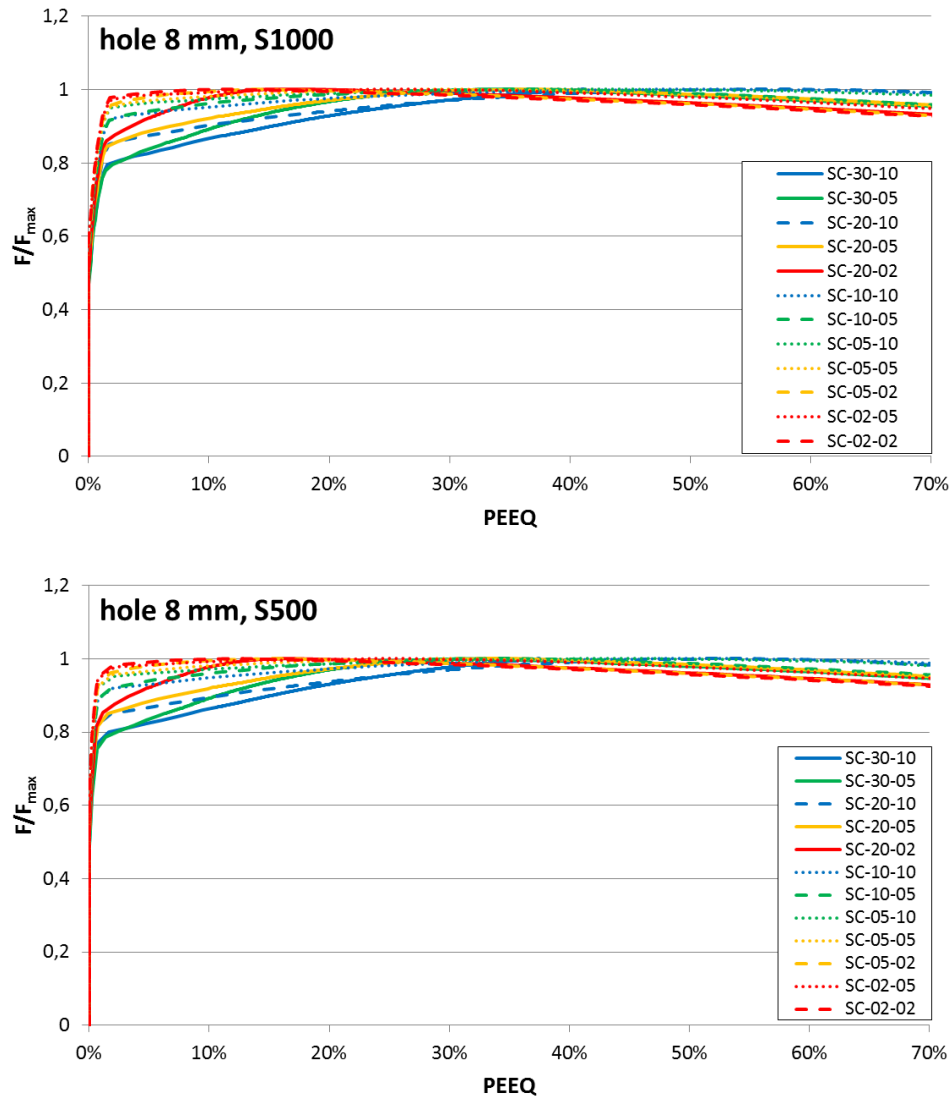


Figure 42. F vs. equivalent plastic strain (PEEQ) for centre hole flat bars with hole 8 mm. Materials with $f_y = 1000$ MPa and $f_y = 500$ MPa.

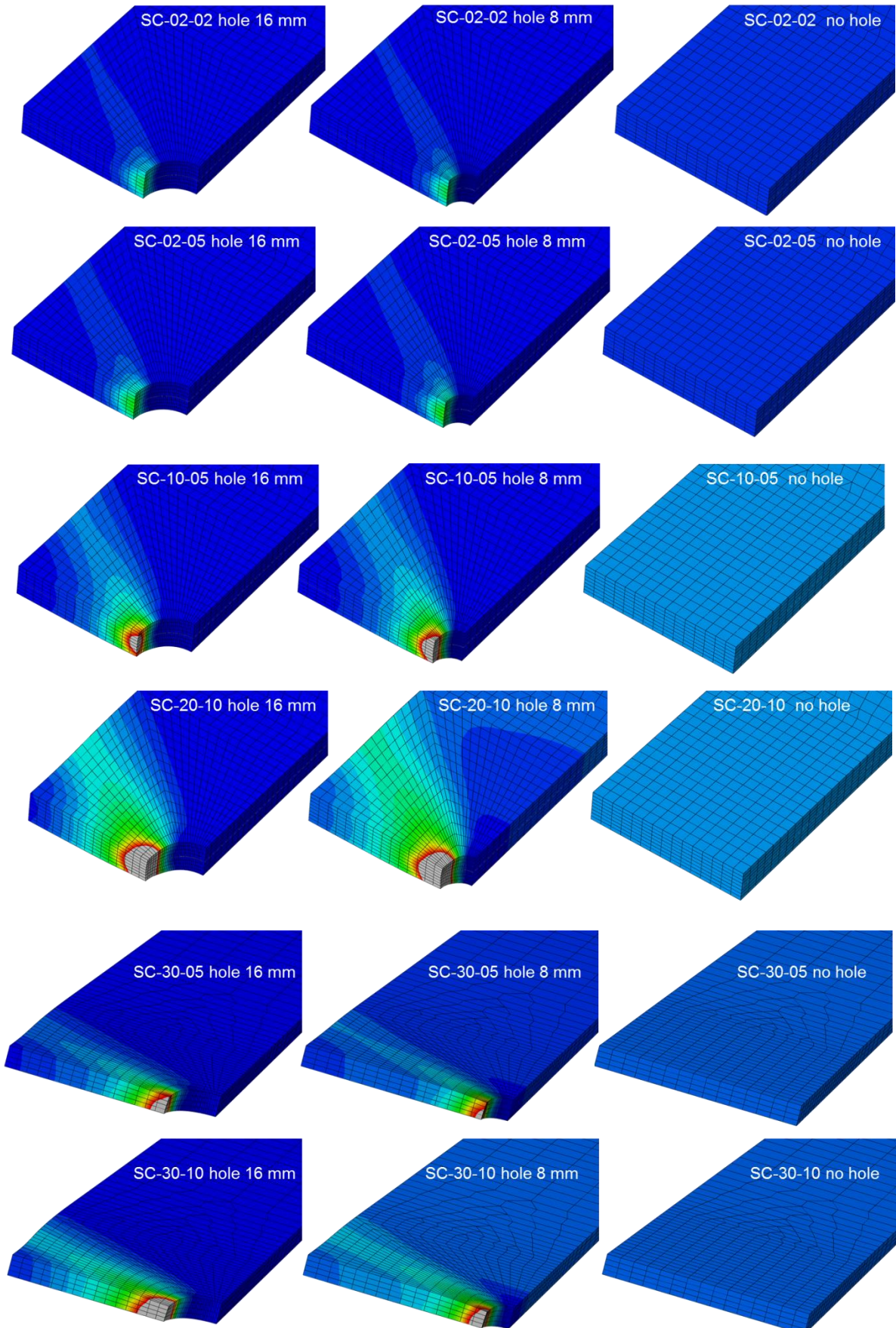


Figure 43. Examples of equivalent plastic strains (PEEQ) at the moment of maximum force. In all pictures dark blue colour presents PEEQ = 0 and grey colour presents PEEQ ≥ 25%.

8. Material ductility requirements for the validity of the results

In the studies with modified material properties the point of maximum force and displacement taken from load-displacement curve has been used as the failure criterion (see Chapter 6.2). This approximation is conservative if the materials can tolerate the equivalent plastic strains at that moment.

The validity study is based on the assumption that that the equivalent plastic strains (ε_{eq} , PEEQ), achieved at the A5 elongation of tensile coupon (gauge length $L_0 = 5.65 \sqrt{A}$), can be accepted in the specimens with holes (Figure 44). This assumption can be considered reliable, because the stress triaxiality at the failure of the specimen with a hole is smaller than the stress triaxiality in the middle of a tension test coupon, and because the relation between failure strain and stress triaxiality can usually be approximated by a monotonic decreasing function (Hradil & al. 2015). If a more accurate solution is desired, it has to be based on rather complicated testing programme.

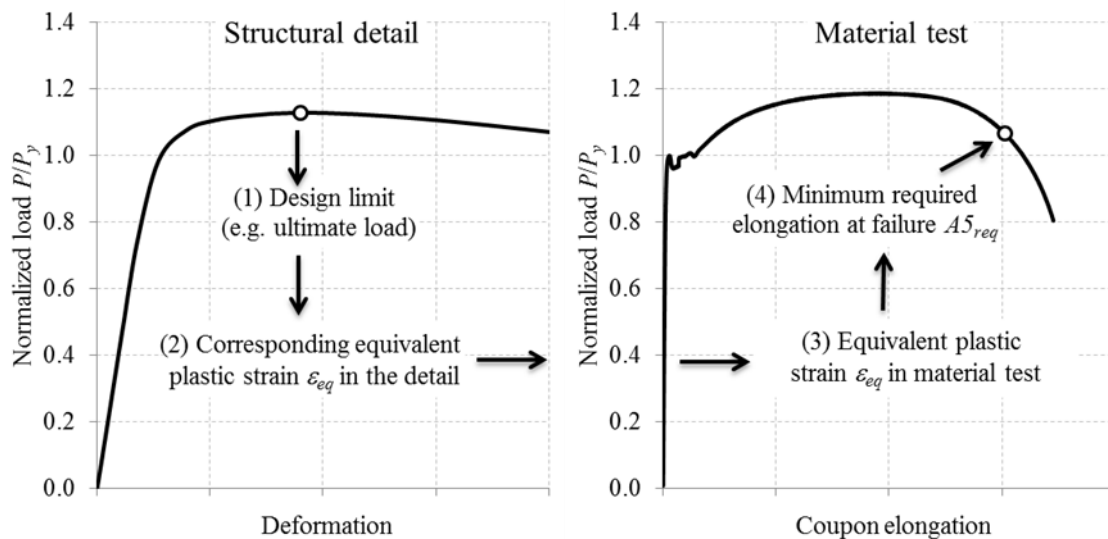


Figure 44. Prediction of minimum required elongation at failure (Hradil & al. 2015).

For determining the A5 elongations corresponding to the utilized maximum plastic strains PEEQ in this study, the tension coupons were modelled ($A = 8 \text{ mm} \times 20 \text{ mm}$). The simulated coupon test had about the same mesh density as the specimens with holes.

Table 17 and Figure 45 summarize the maximum required plastic strains PEEQ utilized in this study and the corresponding necking capacity ($A5-\varepsilon_u$) in material tests. It can be concluded that the results outlined above are valid if A5 is at least 6% higher than uniform elongation. The most critical case is the beam with material model SC-05-05 and $f_y = 500 \text{ MPa}$ (required plastic strains PEEQ = 77%).

Table 17. Maximum required plastic strains PEEQ utilized in this study and corresponding necking capacity ($A5-\epsilon_u$) in material tests. PEEQ values are the larger values of holes 8 mm and 16 mm.

	$f_y = 1000 \text{ MPa}$				$f_y = 500 \text{ MPa}$			
	Beam		Flat bar		Beam		Flat bar	
	PEEQ	$A5-\epsilon_u$	PEEQ	$A5-\epsilon_u$	PEEQ	$A5-\epsilon_u$	PEEQ	$A5-\epsilon_u$
SC-20-10	64%	4.7%	57%	4.2%	69%	5.2%	53%	4.1%
SC-30-10	–		56%	4.2%	–		53%	4.1%
SC-10-10	57%	4.2%	49%	3.6%	61%	4.6%	50%	3.8%
SC-05-10	49%	3.4%	43%	3.0%	44%	3.1%	50%	3.6%
SC-30-05	–		40%	3.6%	–		36%	3.4%
SC-20-05	–		37%	3.4%	–		35%	3.3%
SC-10-05	54%	4.5%	37%	3.3%	55%	4.8%	36%	3.3%
SC-05-05	72%	5.5%	31%	2.7%	77%	6.0%	31%	2.7%
SC-02-05	49%	3.8%	24%	1.8%	45%	3.7%	24%	1.9%
SC-20-02	–		16%	1.8%	–		18%	2.1%
SC-05-02	65%	5.3%	14%	1.5%	64%	5.6%	16%	1.8%
SC-02-02	4%	4.2%	11%	1.1%	38%	3.6%	12%	1.2%

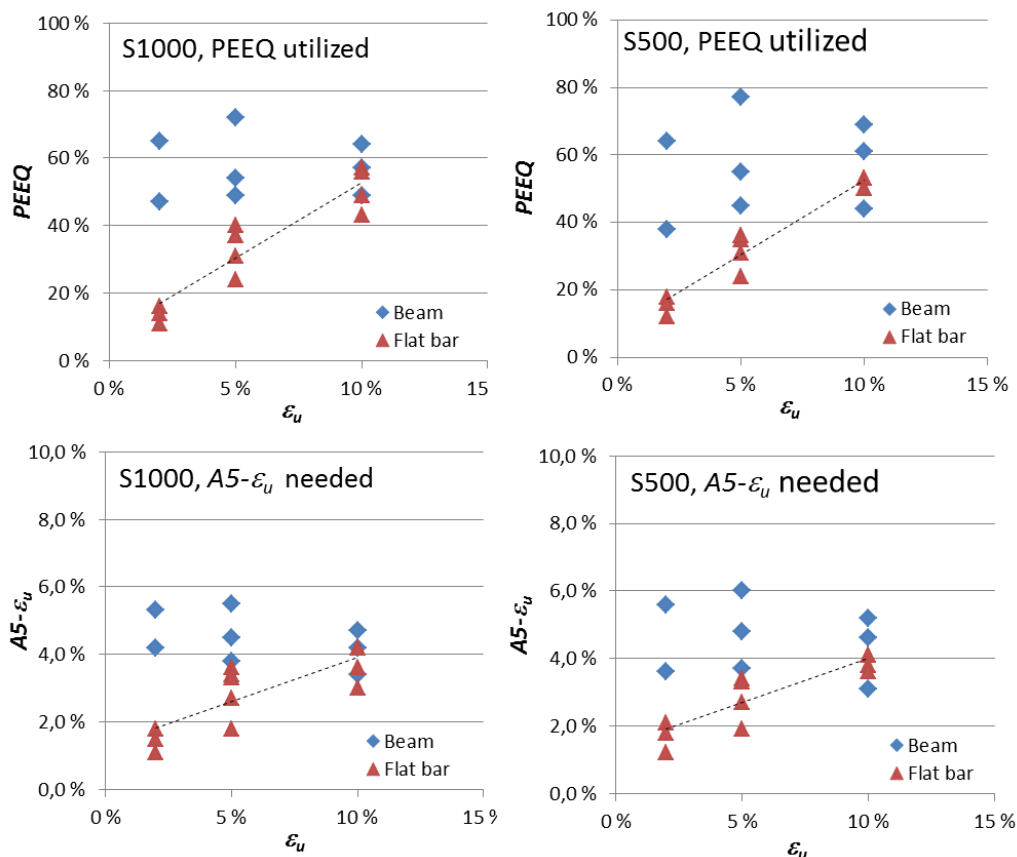


Figure 45. Maximum required plastic strains PEEQ utilized in this study (top graphs) and needed necking capacity ($A5-\epsilon_u$) in material tests to achieve the utilized PEEQ (bottom graphs).

9. Summary and conclusions

Virtual testing of a beam under uniform bending and a flat plate under tension was carried out. Two hole sizes and two material strengths with different material models were under consideration. Tri-linear true stress-true plastic strain material with no strain hardening after the ultimate tensile strength was adopted in the analysis.

9.1 Test matrix for virtual testing

A beam and a flat bar (Figure 46) was tested virtually by ABAQUS. The specimens were calculated without hole and with holes of 8 mm and 16 mm. In the case of beam the holes were only in the bottom flange. Based on the symmetry conditions a quarter of both specimens with length of $L = 500$ mm was modelled. The beam was loaded by end rotation, resulting in uniform bending moment along the beam; and flat bar by axial end displacement. The flat bar presents a borderline case of a beam with a zero web thickness. Materials with $f_y = 1000$ MPa and $f_y = 500$ MPa were studied. $E = 210$ GPa was used in all calculations. Three-stage material model with parameters shown in the table of Figure 46 were used for material modelling. Stages are elastic stage up to f_y , strain-hardening stage up to f_u and ideal plastic stage after f_u . It means that no strain hardening was used in true-stress strain curve after ϵ_u .

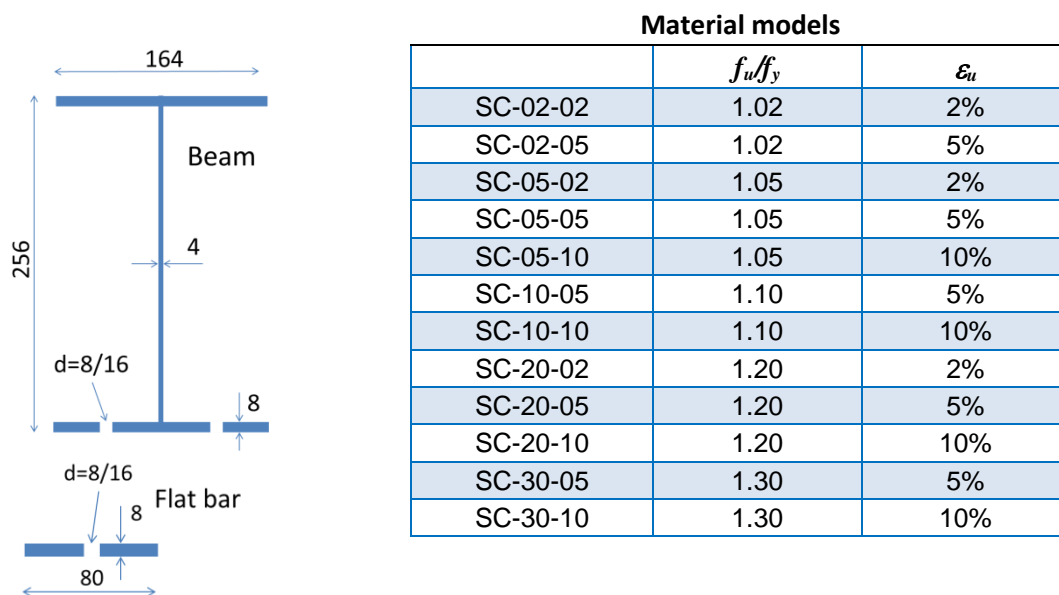


Figure 46. Cross section of the beam and flat bar models and a table of used material model parameters.

The point of maximum force and displacement taken from load-displacement curve has been used as the basis for comparison. This is a conservative assumption, because the descending part of the curve is not utilized in the calculation of rotation capacity R . However, the approximation is valid only if the materials can tolerate the plastic strains at that stress level. Therefore it is required that A5 elongation (gauge length $L_o = 5.65 \sqrt{A}$) in material testing shall be at least 6% larger than the uniform elongation. It means that the necking capacity shall be at least 6%. The conclusion is based on comparison of the plastic strains in holed specimens with the strains in modelled standard tensile coupons.

9.2 Verification of net and gross cross section resistances

According to Eurocodes the design resistance of beams with Class 2 cross sections is based on net cross section properties. Then the resistance shall be greater than

$$M_{c,Rd} = \frac{W_{pl,net} f_y}{\gamma_{M0}}; \gamma_{M0} = 1.0$$

For tension members with holes the resistance shall be greater than both values

$$N_{pL,Rd} = \frac{A f_y}{\gamma_{M0}}; \gamma_{M0} = 1.0 \text{ and } N_{u,Rd} = \frac{0.9 A_{net} f_u}{\gamma_{M2}}; \gamma_{M2} = 1.25$$

The best estimate for resistance in virtual testing is achieved by using ultimate resistance (Figure 47) which is determined by

$$M_u = W_{pl,net} \cdot f_u \text{ for beam model}$$

$$F_u = A_{net} \cdot f_u \text{ for flat bar model}$$

However, especially in the case of flat bars, a small reduction is necessary.

$$F_{u,r} = \frac{F_u}{k_r}; k_r = 1 + 0.1 \left(\frac{f_u}{f_y} - 1 \right)$$

The reduction is significant only in the case of high f_u/f_y ratios (e.g. 3% for $f_u/f_y = 1.3$). If f_y is used in the comparison, as may be used for beams with Class 2 cross sections, factor k_r is not needed. However, then the results are very conservative in the case of large f_u/f_y ratios.

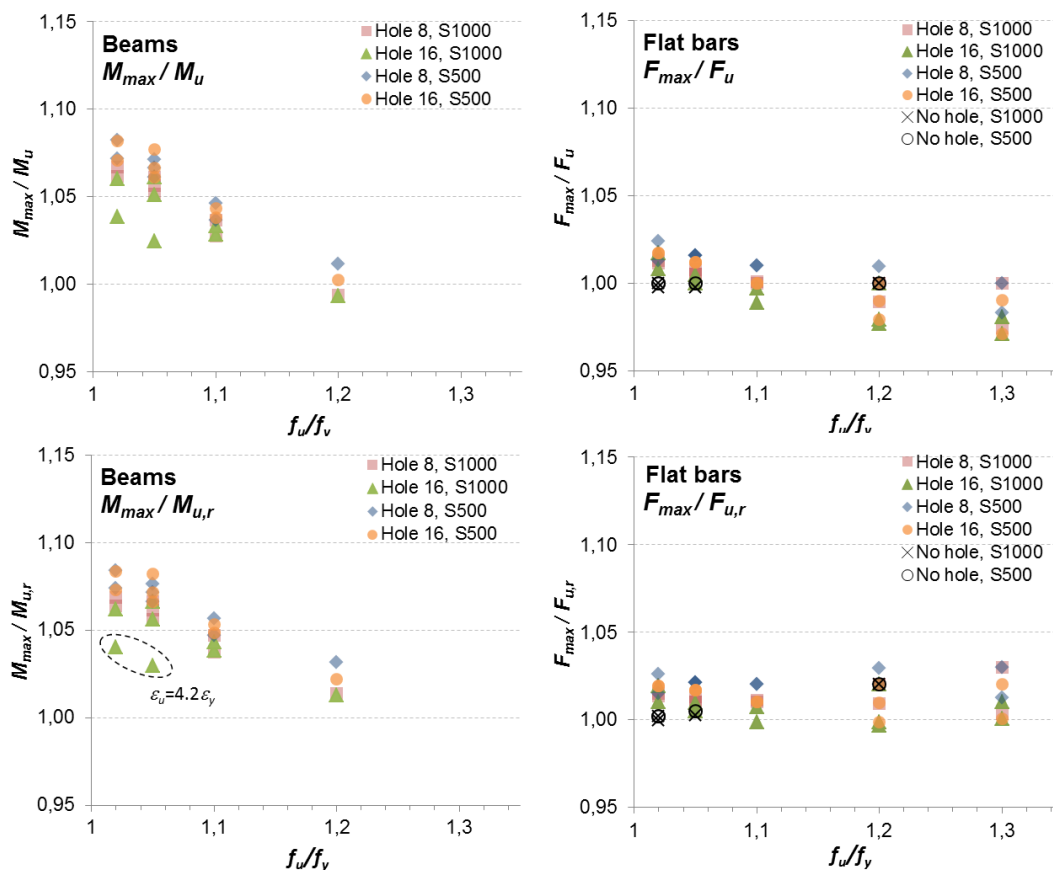


Figure 47. Results for net section resistance (Class 2).

It is worth noting in that when uniform elongation is relatively low ($\epsilon_u = 4.2 \epsilon_y$ for material S1000 with $\epsilon_u = 2\%$), the results (materials SC-02-02 and SC-02-05 in Figure 47) deviate from other results. The deviation cannot be seen in the case of flat bars.

Interestingly, net cross-section together with ultimate tensile strength can be used also to predict the bending resistance of beams. Some tests of relatively compact RHS beams (Ma & Havula 2015) support this rule (Table 18, $M_{max}/M_{pl} \approx f_u/f_y$). The tests were made for non-holed beams. The strength class of the steel was S700.

Table 18. Test results for S700 rectangular hollow sections (Ma & Havula 2015).

Dimensions	f_y	f_u	A5	f_u/f_y	M_{max}/M_{pl}	R
RHS 160x160x10	743 MPa	869 MPa	15.0%	1.17	1.19	3.6
RHS 150x150x8	746 MPa	841 MPa	14.7%	1.13	1.13	2.8

According to Eurocodes the design resistance of beams with Class 1 cross sections is based on gross cross section properties. Then the resistance shall be greater than

$$M_{c,Rd} = \frac{W_{pl}f_y}{\gamma_{M0}}; \gamma_{M0} = 1.0$$

Concerning the fastener holes in the tension, the holes may be ignored provided that for the tension flange

$$\frac{0.9A_{net}f_u}{\gamma_{M2}} \geq \frac{A_gf_y}{\gamma_{M0}}; \gamma_{M0} = 1.0, \gamma_{M2} = 1.25$$

Therefore the results of the beams in virtual testing are compared with the condition

$$M_{max} \geq M_{pl} = W_{pl} \cdot f_y$$

For the flat bars the corresponding condition is

$$F_{max} \geq F_{pl} = F_y = A_g \cdot f_y$$

The comparisons (Figure 48) show following results:

- In the case of beam, condition $M_{max} \geq M_{pl}$ is fulfilled in all cases if $f_u/f_y > W_{pl}/W_{pl,net}$ ($W_{pl}/W_{pl,net} = 1.05$ for hole 8 mm and $W_{pl}/W_{pl,net} = 1.10$ for hole 16 mm). Dashed lines in Figure 48 show that for the border line case when $f_u/f_y = W_{pl}/W_{pl,net}$, the results are 3–7% conservative.
- In the case of flat bar, condition $F_{max} \geq F_y$ is fulfilled almost in all cases if $f_u/f_y > A_g/A_{net}$ ($A_g/A_{net} = 1.11$ for hole 8 mm and $A_g/A_{net} = 1.25$ for hole 16 mm). However, in the case of high f_u/f_y ratios, slightly reduced resistance $F_{y,r} = F_y/k_r$ is required.

It can be concluded that if A_g/A_{net} or $W_{pl}/W_{pl,net}$ is greater than $k_r \cdot f_u/f_y$, Eurocode Class 2 requirement is always fulfilled. For the considered case of I beam this approximation is about 5% conservative, but for flat bars the condition is quite accurate (Figure 48).

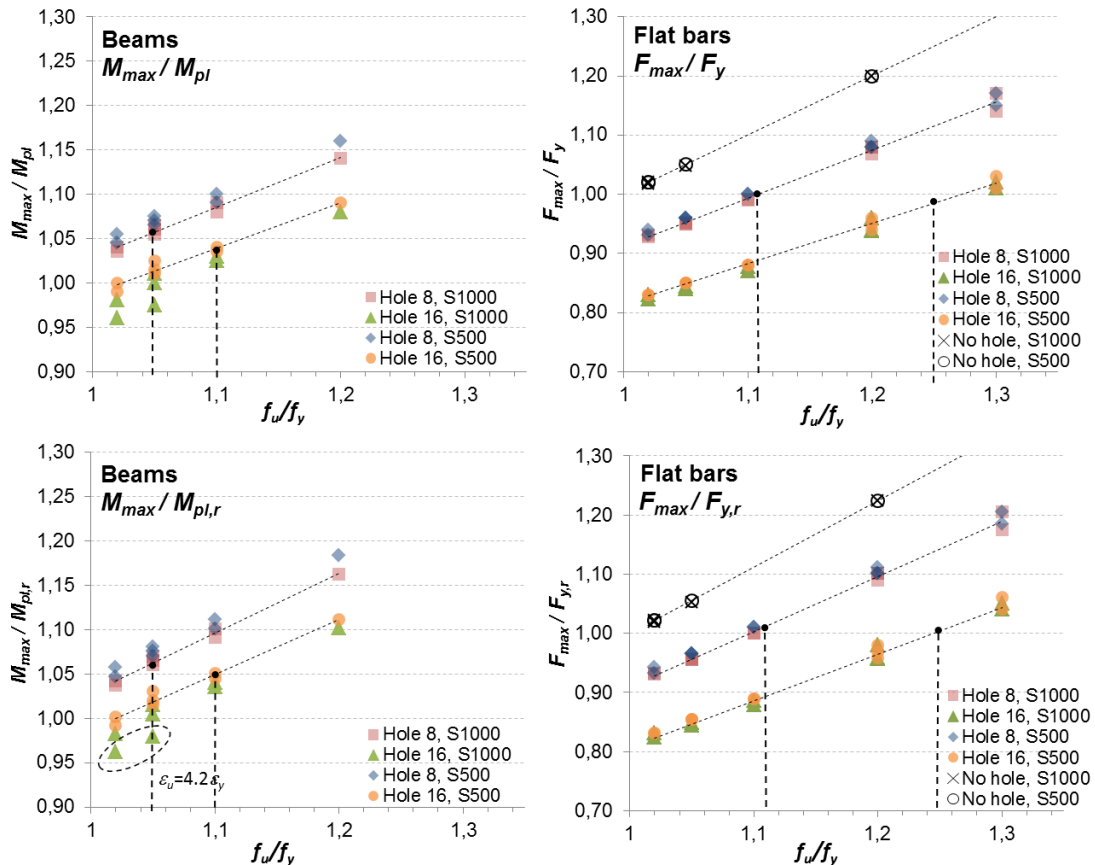


Figure 48. Results for gross cross section resistance (Class 1). The vertical dashed lines show the lower limit of condition $f_u/f_y \geq W_{pl}/W_{pl,net}$ and $f_u/f_y \geq A_g/A_{net}$ for holes 8 mm and 16 mm.

9.3 Verification of rotation capacity

Eurocode requirement for the rotation capacity of beams with Class 1 cross section is

$$R = \frac{\varphi_{max}}{\varphi_{pl}} - 1; \quad \varphi_{pl} = \frac{M_{pl}L}{EI}; \quad M_{pl} = W_{pl}f_y$$

It is based on gross cross section properties. The given rotation φ_{pl} is valid for a beam with uniform bending moment.

Correspondingly, the lengthening capacity of the flat bar is determined by

$$R_t = \frac{\varepsilon_{max}}{\varepsilon_y} - 1 = \frac{\Delta_{max}}{\Delta_y} - 1; \quad \Delta_y = L \frac{f_y}{E}$$

Here a conservative approach where the maximum point of load-displacement curves is used in determination of R and R_t . For the case flat bars without hole $\varepsilon_{max}/\varepsilon_y = \varepsilon_u/\varepsilon_y$. Therefore the condition $R \geq 3$ is always fulfilled (Figure 49) in the cases when the calculation has been continued until elongation $L \cdot \varepsilon_u$.

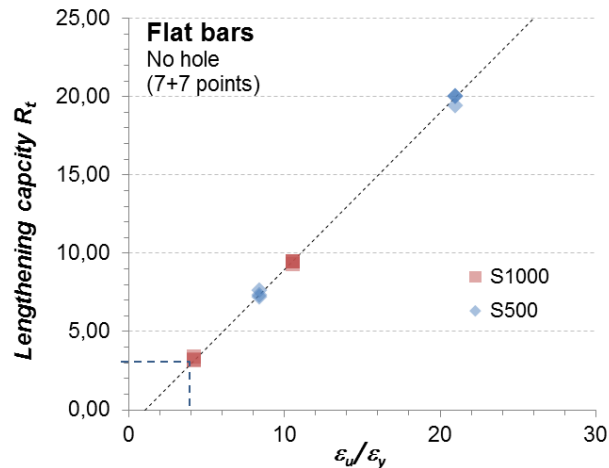


Figure 49. Results for flat bars without holes. The graph includes only the cases in which the calculation has been continued until elongation $L \cdot \epsilon_u$.

Virtual testing of specimens with holes show following results (Figure 50):

- In the case of beams, condition $R \geq 3$ is fulfilled in all cases if $M_{max} \geq 1.08 M_{pl}$.
- In the case of flat bars, condition $R_t \geq 3$ is fulfilled in all cases if $F_{max} \geq 1.09 F_y$.
- If M_{max} or F_{max} is estimated by reduced net section resistance $M_{u,r}$, or $F_{u,r}$, the results are slightly more conservative, then shall be $M_{u,r} \geq 1.07 M_{pl}$ and $F_{u,r} \geq 1.06 F_y$.

It can be concluded that Eurocode Class 1 requirement for $R \geq 3$ is fulfilled if $W_{pl,net} f_u \geq 1.1 W_{pl} f_y$ for the beam or $A_{f,net} f_u \geq 1.1 A_f f_y$ for the tension flange.

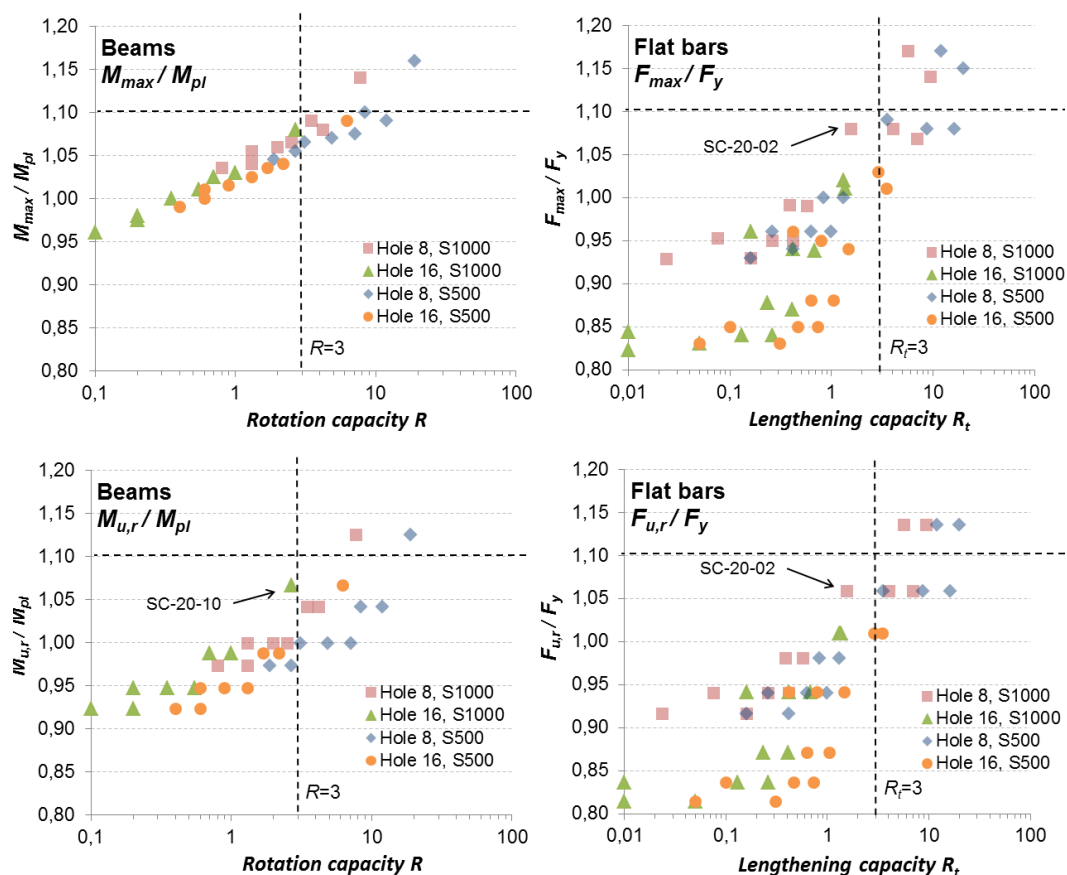


Figure 50. Results for rotation capacity of beams and lengthening capacity of flat bars.

9.4 Main conclusions

Material ductility requirements of beams with flange holes were verified by virtual testing. Local buckling of the compressed parts was prevented by restraints. Tri-linear stress-strain material behaviour with elastic stage up to yield stress f_y , strain-hardening stage up to ultimate strength f_u and ideal plastic stage after f_u was used in true stress-strain material model. Materials with f_u/f_y from 1.02 to 1.30 and ε_u from 2 to 10%, and strengths of $f_y = 1000$ MPa and $f_y = 500$ MPa were under consideration. The requirements for uniform elongation (ε_u) and elongation at fracture (A5) were determined from the results.

Beams without holes:

Conditions given for the cross section classification in Eurocodes, which are in fact set for limiting the slenderness of compression plates in the cross section, were used as the basis of the study. The conditions for cross section classes Class 1 and Class 2 comprise conditions for bending resistance, rotation capacity and net section resistance.

The basic starting point of the study is a beam without holes. Then, the first requirement of Class 1 and Class 2 is that the plastic moment resistance $M_{pl} = W_{pl}f_y$ shall be achieved. The study in Chapter 2.2 indicates that for $f_u/f_y \geq 1.02$, uniform elongation of $\varepsilon_u \geq 6\varepsilon_y$ is adequate for usual I beams and hollow sections, to reach M_{pl} . However, with higher f_u/f_y ratio, even with lower values of ε_u it is possible to reach the requirement. Class 2 cross sections, which do not have additions that do not have conditions for rotation capacity, may have lower requirement for ε_u too.

A second Eurocode requirement specifically for Class 1 is that the plastic rotation capacity $R = 3$ shall be achieved. The study in Chapter 2.1 indicates that in the case of usual I beams and hollow sections with any shape, uniform elongation of $\varepsilon_u \geq 6\varepsilon_y$ results in adequate rotation capacity to fulfil Class 1 cross sections conditions too.

Beams with flange holes:

The virtual testing of beams with flange holes is based on the condition that a specimen with the holes shall tolerate the same equivalent plastic strains as a tension test coupon in standard material testing. Based on the study in Chapter 8, the elongation at fracture (A5 elongation) shall be at least 6% higher than the uniform elongation ε_u , to fulfil the condition.

In the case of beams with flange holes the condition of Class 2 is that the plastic moment net section resistance $M_{pl} = W_{pl,net} f_y$ shall be achieved in net cross section. The study in Chapter 9.2 shows that all virtual tests fulfil this condition.

In the case of Class 1 sections, an additional requirement is necessary for the net section resistance. This ensures that sufficient plastic elongations, resulting in the rotation capacity $R \geq 3$, develop in the gross cross section before the net section fails. The results in Chapter 9.2 show that the condition $M_u \geq 1.1M_{pl}$ is necessary to fulfil this requirement. Then the ultimate bending resistance of the net section is determined by $M_u = W_{pl,net} f_u$ and plastic bending resistance by $M_{pl} = W_{pl} f_y$.

The results above indicate that Eurocode requirements are too conservative for beams with flange holes. In Eurocodes the material requirements are for uniform elongation $\varepsilon_u \geq 15\varepsilon_y$ and for fracture elongation $A5 \geq 10\%$ (see Chapter 2.3). Also the requirement concerning the fastener holes in the tension flange of Class 1 cross sections seem to be too conservative, when the partial safety factor $\gamma_{M0} = 1.25$ is applied together with additional reduction factor of 0.9 (see Chapter 9.2).

9.5 Some remarks on the results

It should be noted that this study is based on a beam with a flange hole and a uniform bending moment. Therefore in the case of other loading conditions or structural details the results may be different. In the case of localised plastic deformations, the rotation capacity depends also on dimensions and loading arrangements of the beam. Large deformations in the areas of local discontinuities or other type of large secondary effects (tolerances, residual stresses, sharp notches, etc.) may have different impact on the material ductility requirements than an ideal hole in tension flange has.

The most significant parameter affecting rotation capacity is the ratio of $\varepsilon_u/\varepsilon_y$. Therefore, for a fixed R and ε_u , required plastic rotations are the larger the higher is f_y . More favourable in the case of high strength steels should be to use required plastic rotation φ_{req} instead of R .

The net section resistance is proportional to f_u . The lower is f_u/f_y the more difficult is the yielding of the gross cross-section outside net cross section. Therefore materials with low f_u/f_y are more sensitive to net section failure.

In a general sense the conditions presented above for a hole do not alone guarantee adequate deformation capacity at other type of local discontinuities. The deformation capacity depends on the level of local plastic strains and material-dependant critical plastic strains.

References

- AISC. 2010. ANSI/AISC 360: Specification for Structural Steel Buildings. American Institute of Steel Construction.
- AISI S100. 2007. North American specification for the design of cold-formed structural members.
- Arasaratnam, P. 2008. Effects of Flange Holes on Flexural Behavior of Steel Beams. Thesis for Degree of Doctor of Philosophy. McMaster University, Ontario, Canada. 376 p.
- Chopra, A. K., Newmark, N. M. 1980. Design of Earthquake Resistant Structures. John Wiley and Sons, New York, New York, USA.
- Dexter, R.J., Altstadt, S.A., Gardner C.A. 2002. Strength and Ductility of PS70W Tension Members and Tension Flanges with holes. University of Minnesota.
- Driscoll, G. C.1958. Rotation Capacity Requirements for Beams and Portal Frames. PhD Thesis, Lehigh University, Bethlehem, Pennsylvania, USA.
- EN 1993-1-1. 2005. Eurocode 3: Design of steel structures - Part 1-1: General rules and rules for buildings. European Committee for Standardization, Brussels.
- EN 1993-1-12. 2007. Eurocode 3 - Design of steel structures - Part 1-12: Additional rules for the extension of EN 1993 up to steel grades S 700. European Committee for Standardization, Brussels.
- Eurocode 3 Editorial Group. 1989. The b/t Ratios Controlling the Applicability of Analysis Models in Eurocode 3, Document 5.02, Background Documentation to Chapter 5 of Eurocode 3, Aachen University, Germany.
- Hradil, P., Talja, A. 2015. True Stress-Strain Relationship for Finite Element Simulation of Structural Details Under Diffuse Necking, Nordic Steel Construction Conference 2015.

- Hradil, P., Fülöp, L., Talja, A., Ongelin P. 2015 Ductility requirements for details with stress concentration and diffuse necking. SDSS2016: International Colloquium on Stability and Ductility of Steel Structures. Manuscript 5.10.2015.
- Giouncy. V. 2000. Framed structures. Ductility and seismic response. General Report. Journal of Constructional Steel Research 55 (2000) 125–154.
- Gioncu. V. Petcu. D. 1997. Available Rotation Capacity of Wide-Flange Beams and Beam-Columns. J. Construct. Steel Res. Vol. 43. Nos. 1-3. pp 161–217.
- Hasan, S. W., Hancock, G. J. 1988. Plastic Bending Tests of Cold-Formed Rectangular Hollow Sections. Research Report, No R586, The University of Sydney.
- Kerfoot, R., P. 1965. Rotation Capacity of Beams. Fritz Engineering Laboratory Report No 297.14, Lehigh University, Bethlehem, Pennsylvania, USA.
- Korol, R. M., Hudoba, J. 1972. Plastic Behaviour of Hollow Structural Sections. Journal of the Structural Division, American Society of Civil Engineers, Vol 98, No ST5, pp 1007–1023.
- Ma, Z. Havula J. 2015. Bending tests of S700 tubes. HAMK Sheet Metal Centre Report No. 2015-56. Häme University of Applied Sciences (HAMK), Hämeenlinna.
- Mazzolani FM.. Piluso V. 1997. Prediction of the Rotation Capacity of Aluminium Alloy Beams. Thin-Walled Structures Vol. 27. No. 1. 103–116.
- RFCS.1998. Background document to Eurocode 3 about ductility evaluation of plastic hinges. Annex 12 of Report EUR 18366: Promotion of plastic design for steel and composite cross-sections; new required conditions in Eurocodes 3 and 4, practical tools for designers. Luxembourg: Office for Official Publications of the European Communities.
- Shokouhian. M., Shi. Y. 2014. Classification of I-section flexural members based on member ductility. Journal of Constructional Steel Research 95 (2014) 198–210.
- Talja, A. Hradil, P. 2015. Ductility limits of high strength steels, VTT Research Report VTT-R-02599-15.
- Wilkinson, T., Hancock G.J. 1998. Compact or Class 1 Limits for Rectangular Hollow Sections in Bending. Tubular Structures VIII, Proceedings, 8th International Symposium on Tubular Structures, Singapore, August 1998, pp 409–416.
- Wilkinson, T. 1999. The plastic behaviour of cold-formed rectangular hollow sections. Thesis for Degree of Doctor of Philosophy. The University of Sydney.
- Yura, J. A., Galambos, T. V., Ravindra, M. K. 1978. The Bending Resistance of Steel Beams, Journal of the Structural Division, Proceedings of the American Society of Civil Engineers, Vol 104, No ST 9, September, 1978, pp 1355–1370.
- Zhao, X. L., Hancock, G. J. 1991. Tests to Determine Plate Slenderness Limits for Cold-Formed Rectangular Hollow Sections of Grade C450. Steel Construction, Journal of Australian Institute of Steel Construction, Vol 25, No 4, November 1991, pp 2–16.